FHV
Vorarlberg University
of Applied Sciences

Development of a Software Tool to calculate the Channel Spacing of an optical Multiplexer/ Demultiplexer based on Arrayed Waveguide Gratings in accordance to ITU-Grid Standards

Master's Thesis
Submitted in Fulfillment of the Degree

Master of Science in Engineering (MSc)

Vorarlberg University of Applied Sciences
Master of Mechatronics

Submitted to
Dr. habil. Dana Seyringer, PhD

Handed in by
Manuel Humpeler, BSc

Dornbirn, September 2022

Abstract

Development of a Software Tool to calculate the Channel Spacing of an optical Multiplexer/Demultiplexer based on Arrayed Waveguide Gratings in accordance to ITU-Grid Standards

In today's world, fiber optic networks for data transmission are an essential technology. This technology provides multiple advantages compared to conventional electrical data transmission. The simultaneous transmission of multiple optical signals in a single fiber is one of the main benefits of fiber optic cable. This is accomplished by directing the different optical signals into a single fibre and splitting them up after the transmission in order to obtain the individual signals. Arrayed Waveguide Gratings (AWGs) are used for this purpose in modern optical networks. Design and evaluation process are two components of AWG development. During the evaluation of several simulated and already manufactured AWGs for telecommunication applications, it was discovered that the channel spacing parameter does not conform telecommunication standards. The correct shift of the geometric parameter "separation of the output waveguides" leads to the standard-conform channel spacing.

According to the current state of the art, no commercial tool is available which calculates the shift of this parameter correctly. The aim of this thesis is the development of a software tool to calculate the accurate shifting of the geometric parameter "separation of the output waveguides" of an AWG. This tool operates as an interface between the design and evaluation processes and must be able to import the data format of the evaluation process and returns the data in a suitable data format for the design process. The Vorarlberg University of Applied Sciences uses three different methods for the shifting of the geometric parameter "separation of the output waveguides". These methods are evaluated and optimised as part of this thesis. Additionally, it has been determined that the shift of the geometric parameter "separation of the output waveguides" has no significant impact on the performance of the AWG.

Kurzreferat

Entwicklung eines Softwaretools zur Berechnung des Kanalabstands eines optischen Multiplexers/Demultiplexers auf der Basis von Arrayed Waveguide Gratings nach ITU-Grid Standards

In der heutigen Welt sind Glasfasernetze für die Datenübertragung eine unverzichtbare Technologie. Diese Technologie bietet zahlreiche Vorteile im Vergleich zur herkömmlichen elektrischen Datenübertragung. Die simultane Übertragung mehrerer optischer Signale in einer einzigen Faser ist einer der wichtigsten Vorzüge von Glasfaserkabeln. Dazu werden die verschiedenen optischen Signale in eine einzige Faser geleitet und nach der Übertragung in einzelne Signale aufgespalten. In modernen optischen Netzen werden zu diesem Zweck Arrayed Waveguide Gratings (AWGs) eingesetzt. Design und Evaluierung sind zwei Komponenten der AWG-Entwicklung. Bei der Evaluierung mehrerer simulierter und bereits hergestellter AWGs für Telekommunikationsanwendungen wurde festgestellt, dass der Parameter Kanalabstand nicht den Telekommunikationsstandards entspricht. Die korrekte Verschiebung des geometrischen Parameters "Trennung der Ausgangshohlleiter" führt zu einem normgerechten Kanalabstand.

Nach dem aktuellen Stand der Technik ist kein kommerzielles Softwaretool verfügbar, das die Verschiebung dieses Parameters korrekt berechnet. Ziel dieser Arbeit ist die Entwicklung eines Softwaretools zur Berechnung der genauen Verschiebung des geometrischen Parameters "Trennung der Ausgangshohlleiter" eines AWG. Dieses Tool fungiert als Schnittstelle zwischen dem Design- und dem Evaluierungsprozess und muss in der Lage sein, das Dateiformat des Evaluierungsprozesses zu importieren und die Daten in einem geeigneten Dateiformat für den Designprozess zurückzugeben. Die Fachhochschule Vorarlberg verwendet drei verschiedene Methoden für die Verschiebung des geometrischen Parameters "Trennung der Ausgangshohlleiter". Diese Methoden werden im Rahmen dieser Arbeit evaluiert und optimiert. Darüber hinaus konnte festgestellt werden, dass die Verschiebung des geometrischen Parameters "Trennung der Ausgangshohlleiter" keinen signifikanten Einfluss auf die Leistung des AWGs hat.

Contents

List of Figures

List of Tables

List of Abbreviations and Symbols

MUX Mulitplexer

DEMUX Demulitplexer

WDM Wavelength Division Multiplexing

CWDM Coarse Wavelength Division Multiplexing

DWDM Dense Wavelength Division Multiplexing

HDWDM High Dense Wavelength Division Multiplexing

VHDWDM Very High Dense Wavelength Division Multiplexing

TFF Thin Film Filter

FBG Fibre Bragg Grating

FSDG Free-Space Diffraction Gratings

AWG Arrayed Waveguide Grating

PA Phased Array

PHASARs phased-array grating

WGRs Waveguide Grating Routers

UML Unified Modelling Language

GUI Graphical User Interface

1 Introduction

The globalization of the world and the increasing exchange of information over short and long distances have increased greatly in recent years. The Internet is the most widely used medium for the transmission of data and information. Figure 1.1 shows how much global data transmission has increased from 2017 to the present. In 2017, 100 exabytes of data were sent over the Internet per month. Five years later, 333 exabytes were transferred per month, more than three times as much.

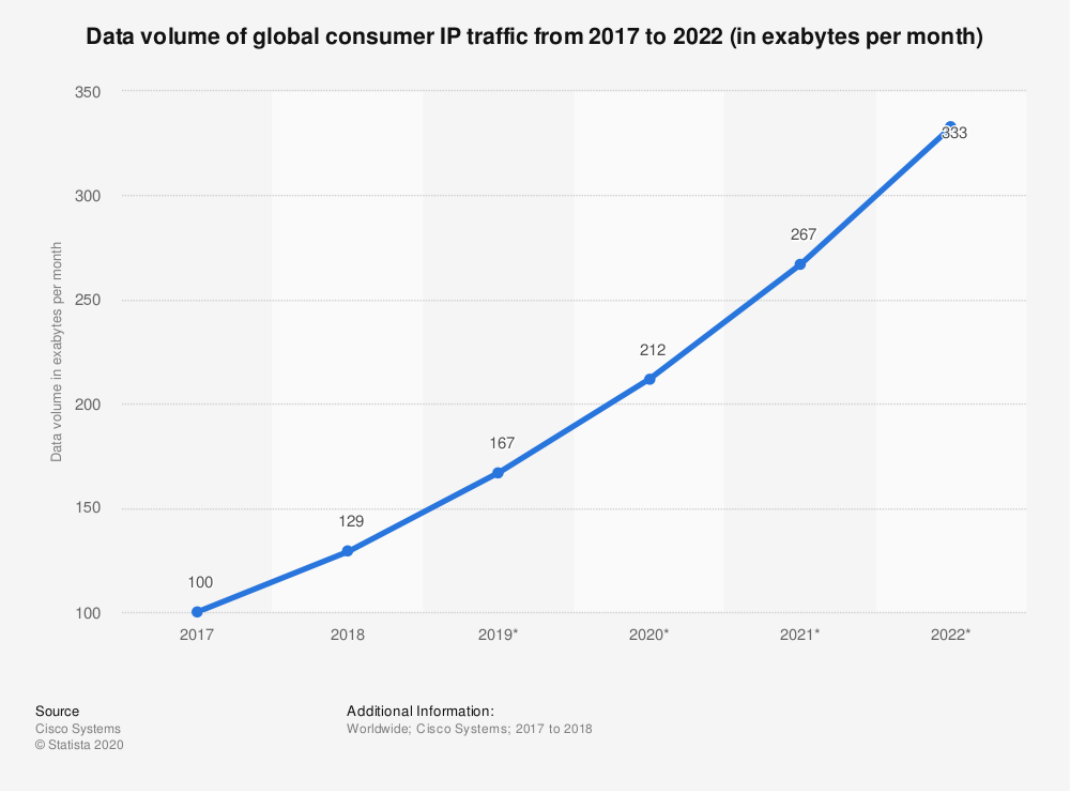

Figure 1.1: Global data traffic [1].

To meet the demands on increasing data volume, a new technology was developed, which is known as fibre optics. This technology has several advantages over conventional electrical data transmission. Fibre optics uses light as the

transmission medium, where each frequency (or wavelength) of light represents an optical signal. One of the advantages of fibre optics is that several optical signals can be transmitted simultaneously in a single fibre. This means the more different frequencies (or wavelengths) are used for transmission, the higher amount of data can be transmitted. By comparison, in an electrical conductor (wire), only one electrical signal can be transmitted at a time [2]. Further advantages of optical data transmission are:

- A coaxial cable (latest development in the electrical data transmission) loses half of its power in the high-frequency range after only a few hundred meters. Optical signals in the fibre require amplification only after approximately 60 km.
- The data rate for a coaxial cable is in the Mb/s range, for fibre optic it is in the Gb/s range.
- Optical data transmission is immune to magnetic interference and is almost noise free.
- Fibre optic cables are lighter and smaller than the electric cables.
- The different light signals, transmitted in the fibre, do not interfere with each other and lead to strong increase in transmission capacity [3].

The next section explains the state of the art of a fibre optic communication.

1.1 State of the Art

As already mentioned in the introduction, the optical data transmission makes it possible to transmit multiple optical signals in a single fibre. On the transmitter side, a Mulitplexer (MUX) is used to combine the different optical signals in the fibre. The resulting mixed optical signal is transported over the fibre. At the receiver end, the individual optical signals are separated with the aid of a Demulitplexer (DEMUX). This technology is called Wavelength Division Multiplexing (WDM).

1.1.1 Wavelength Division Multiplexing

In Figure 1.2 the functional structure of a WDM system is shown. Since computers and servers currently still read, process, and write data (or signals) in the electrical domain, it is necessary for a WDM system to convert the data into an optical signal. At the transmitter end, this is realised with a light source, usually

a laser. The lasers emit each different wavelength $\lambda_1,\ldots,\lambda_n$ for each electrical input signal, where n is the number of input signals (also called transmission channels) in the optical domain. The difference between two adjacent wavelengths is called channel spacing. The wavelengths, used for data transmission, are combined in optical multiplexer to produce a spectrum of light. This signal is transmitted via a single optical fibre. At the receiving end a demultiplexer is used to split the spectrum to obtain the original optical signals $\lambda_1,\ldots,\lambda_n$. Photodetectors are used to convert the optical signals into electrical signals [4].

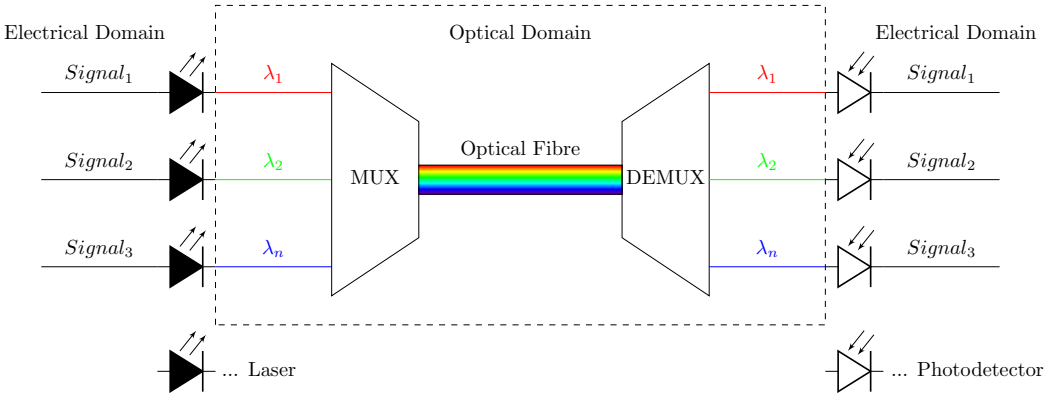

Figure 1.2: Wavelength Division Multiplexing.

1.1.2 Different WDM Systems

There are three different types of WDM systems, which are classified according to how many channels (or input and output signals) the MUX/DEMUX can process:

- **Coarse Wavelength Division Multiplexing (CWDM)** is a method for low-cost and short-distance applications. Up to eight transmission channels can be realised, so the transmission capacity is limited. This is because a larger channel spacing (distance between two adjacent wavelengths) is used, usually 2500 GHz (= 20 nm).
- **Dense Wavelength Division Multiplexing (DWDM)** offers the possibility of 16 to 40 transmission channels. Typically, channel spacing of 100 GHz (= 0.8 nm) or 50 GHz (= 0.4 nm) is selected. This low value requires more precise optical components and is therefore more expensive than CWDM methods.

- **High Dense Wavelength Division Multiplexing (HDWDM)** and **Very High Dense Wavelength Division Multiplexing (VHDWDM)**: As shown in Figure 1.1, the global data rate is increasing enormously. This requires an increase in the number of transmission channels. To achieve this, the channel spacing has to be minimised. With HDWDM or VHDWDM methods, this spacing is 25 GHz (= 0.2 nm), but it can also be as low as 12.5 GHz (= 0.1 nm) or less. This means that 128 or more transmission channels can be realised [5].

1.1.3 Types of optical multiplexing/demultiplexing

Multiplexers and demultiplexers are essential components in a WDM system. The simplest method to realise them is with a prism and lenses, as shown in Figure 1.3. The figure shows the functionality of a demultiplexer. The surface of a prism is struck by a beam of polychromatic light, causing each wavelength to be refracted differently. The wavelengths have split and are shifted by an angle. A lens is used to focus the individual wavelengths onto a guided fibre. To realise a multiplexer the components have to be reversed [1].

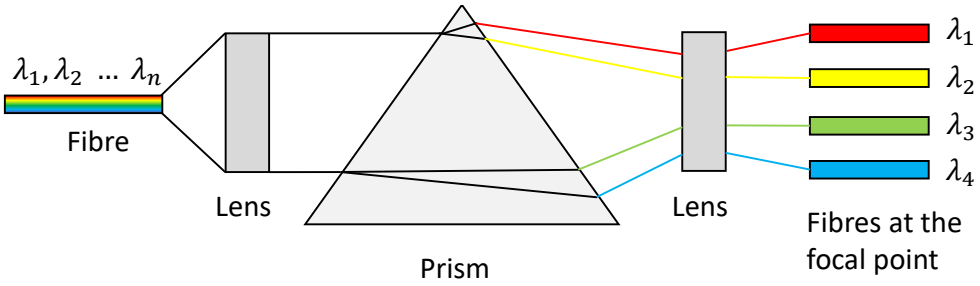

Figure 1.3: Demultiplexer realised with a prism.

Nowadays MUXs/DEMUXs are realised which operate with diffraction and interference. There are two different types that work with these physical properties: serial and parallel MUXs/DEMUXs.

Serial Muliplexer/Demultiplexer

Serial MUX/DEMUX uses physical mechanisms to filter the wavelengths. In this process, the wavelengths are not filtered out simultaneously, instead they are filtered out one after the other. There are two different types of serial multiplexers/demultiplexers: Thin Film Filter (TFF) structure, which is shown in Figure 1.4 and the Fibre Bragg Grating (FBG) structure illustrated in Figure 1.5.

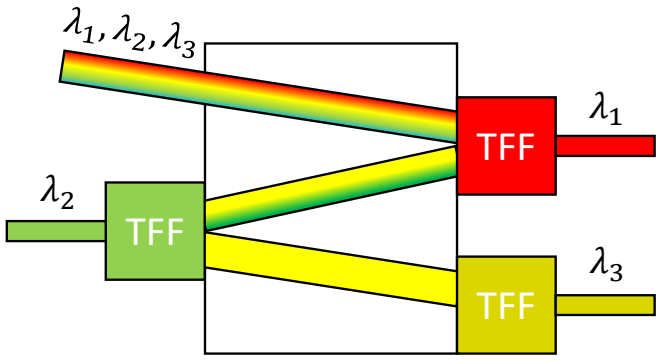

Figure 1.4: Demultiplexer using TFF.

A Thin Film Filter consists of series of alternating layers of a transparent dielectric material with different refractive indices, which are sequentially deposited on an optical substrate. Due to the different refractive indices, a single wavelength can pass through the filter and the others are reflected. The TFF method is generally only used for a small number of transmission channels (16 channels) [6].

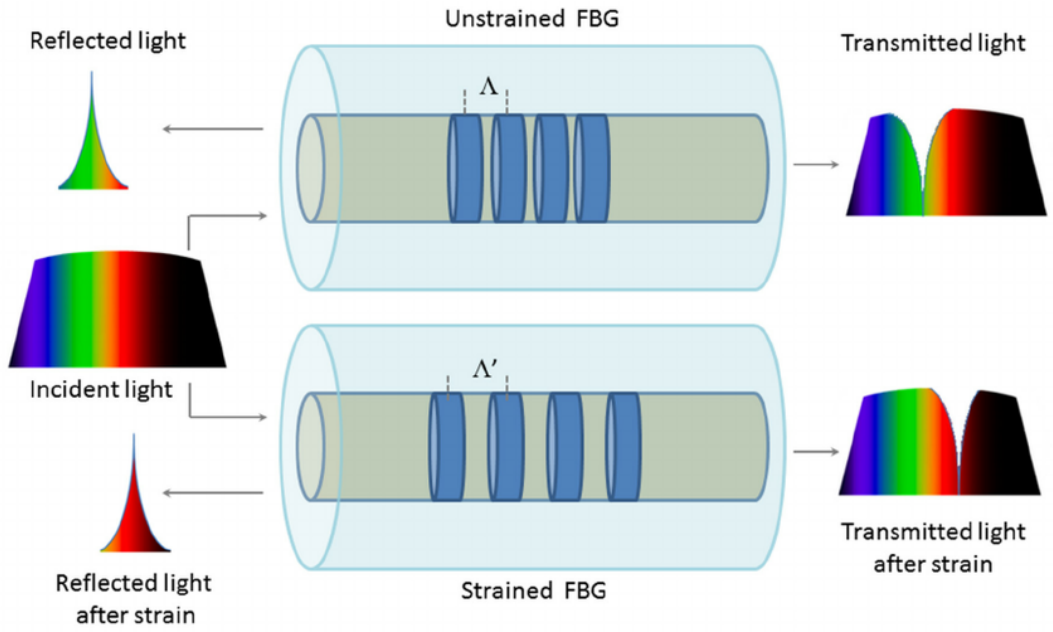

Figure 1.5: Demultiplexer using FBG [7].

FBG is an optical fibre which changes the refractive index in the core of the fibre over its length from a high to a low index. Due to the different refractive indices,

an FBG acts like a mirror that reflects certain wavelengths and transmits others. It depends on the distance Λ between the high and low refractive index regions in the fibre which wavelength is reflected.

Parallel Multiplexer/Demultiplexer

With a parallel multiplexer/demultiplexer, all wavelengths are simultaneously combined or split. This method is used for applications with a higher number of transmission channels. There are two different types: Free-Space Diffraction Gratings (FSDG) and Arrayed Waveguide Grating (AWG). Figure 1.6 shows the structure of an FSDG technology. The polychromatic light wave impinges on the diffraction gratings, causing the individual wavelengths to be offset by a certain angle. The different wavelengths pass through a lens before being directed into a guided fibre [8].

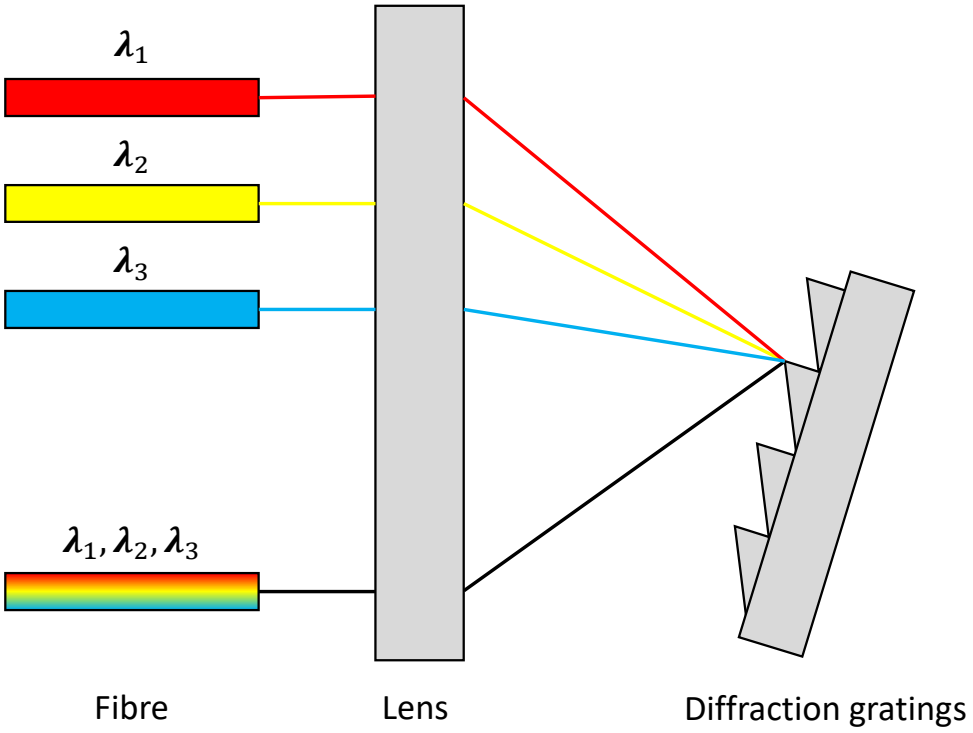

Figure 1.6: Demultiplexer using FSDG.

The functionality of an AWG and its advantages will be covered in the next section.

1.1.4 Arrayed Waveguide Gratings

In the WDM system, the key components are the passive optical multiplexers/demultiplexers. For more advanced applications like DWDM, HDWDM or VHDWDM, Arrayed Waveguide Gratings (AWG) is used for multiplexing and demultiplexing, as it has several advantages over the MUXs/DEMUXs described in Subsection 1.1.3. The main advantages are listed below:

- Simple adjustment of the wavelengths
- Low insertion loss (-3 dB) and cross-talk (-35 dB)
- Suitable for integration with photodetectors
- Large number of transmission channels

AWGs can be classified as phased-array grating (PHASARs) and Waveguide Grating Routers (WGRs) [9].

1.1.4.1 AWG Principle

An AWG structure consists of the following components: input/output waveguides, two couplers, and an array of waveguides (also called Phased Array (PA)) which are shown in Figure 1.7. The optical signal, which consists of multiple wavelengths, λ_1 - λ_n, is coupled into the input waveguide from a single fibre. The input coupler must have a certain length, *Lf*, so that the light is distributed over the waveguides in the phased array (where *Na* parameter defines the number of PA waveguides). The path length difference, *dL* between adjacent waveguides in the phased array must be chosen so that it is an integer multiple of the central wavelength, λ_c of the AWG demultiplexer, see Figure 1.7 and Figure 1.8. This results in a constant optical path length difference of the waveguides which causes diffraction and interference of the light in the output coupler. The distance between the adjacent PA waveguides is given by parameter *dd*. The individual wavelengths are then focused each on one separated point on the focal line in the output coupler, as shown in Figure 1.7. The parameter *dx* is defined as the separation between two adjacent focus points (separation between output waveguides).

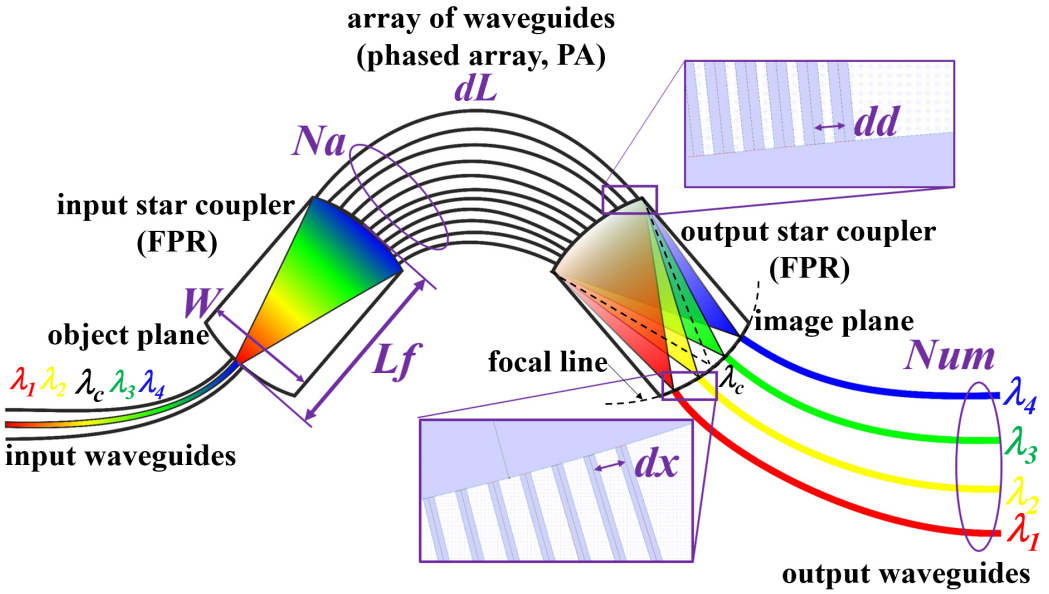

Figure 1.7: Arrayed waveguide gratings [5].

The functionality of an AWG can be categorised by its transmission characteristics. These can either be measured on the real component or determined by the simulation. Vorarlberg University of Applied Sciences [10] uses the commercial photonics tool Phasar from Optiwave [11] for the AWG design and the simulation. Figure 1.8 shows the simulated transmission characteristics of a 20-channel 200-GHz AWG. The horizontal axis shows the insertion losses in dB and the vertical axis shows the wavelengths in nm.

The transmission parameters can be calculated from the transmission characteristics. These parameters describe the performance of an AWG and are relevant for the design, simulation, fabrication and application of an AWG [12].

In general, the development process of an AWG can be divided into design, evaluation and optimisation, whereby the design and evaluation processes are described in the next two sections.

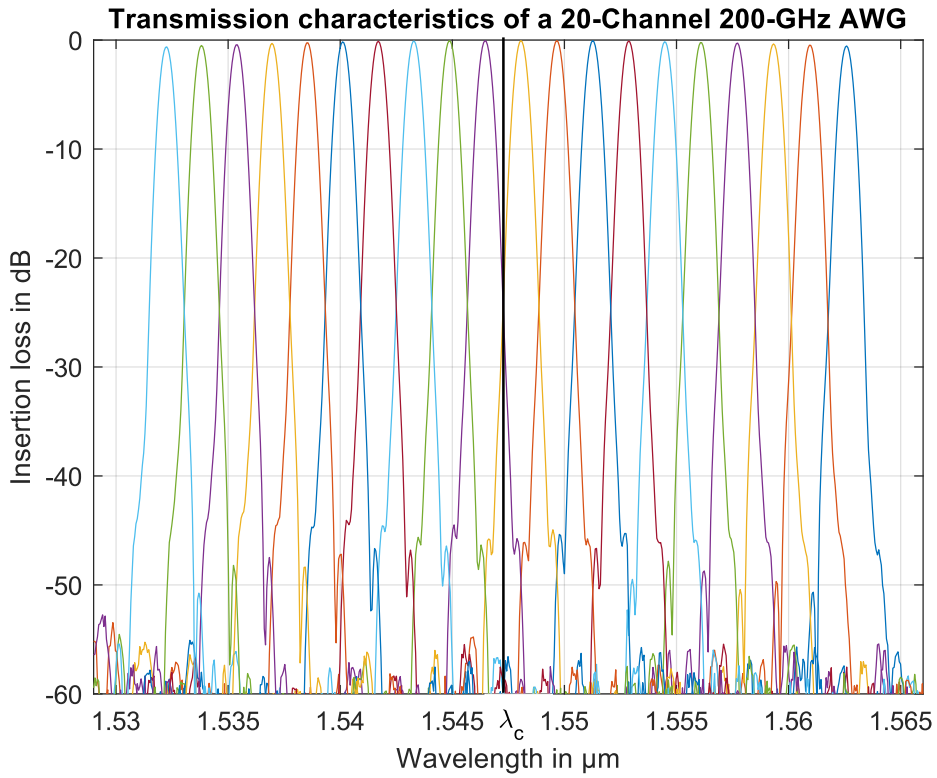

Figure 1.8: Transmission characteristics of a 20-channel 200-GHz AWG.

1.1.4.2 Design Workflow of an AWG

The design of an AWG is a time-consuming process that requires several phases. Figure 1.9 shows the workflow of an AWG design as it is carried out at the Vorarlberg University of Applied Sciences. It starts with the specifications (customer-specific and material parameters) of the AWG required by the customer (input parameters). These parameters are used in the AWG-Wuckler tool [13], which was developed by the Vorarlberg University of Applied Sciences, to calculate the geometric parameters (*dd*, *dx*, *Lf*, *dL* and *Na*) explained in Subsection 1.1.4.1. The design parameters (material and geometric parameters) are the inputs for the commercial tool Phasar from Optiwave. With this tool the AWG can be designed and simulated. The result of the simulation is the transmission characteristics, which is the basis for the evaluation of the designed AWG.

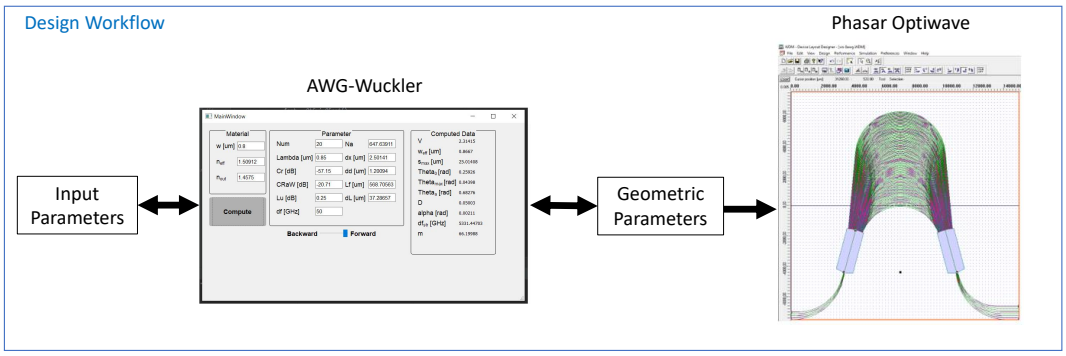

Figure 1.9: Design Workflow of an AWG.

1.1.4.3 Evaluation Workflow of an AWG

To verify whether the design of the AWG complies with the customer requirements, the simulation results need to be evaluated to determine the transmission parameters that specify the quality of the AWG design. The evaluation workflow consists of several phases, as shown in Figure 1.10. By simulating the AWG structure in the Phasar tool, as described before, the transmission characteristics are obtained. With the AWG-Analyzer tool [14], which was also developed at the Vorarlberg University of Applied Sciences, the transmission parameters are calculated from the transmission characteristics.

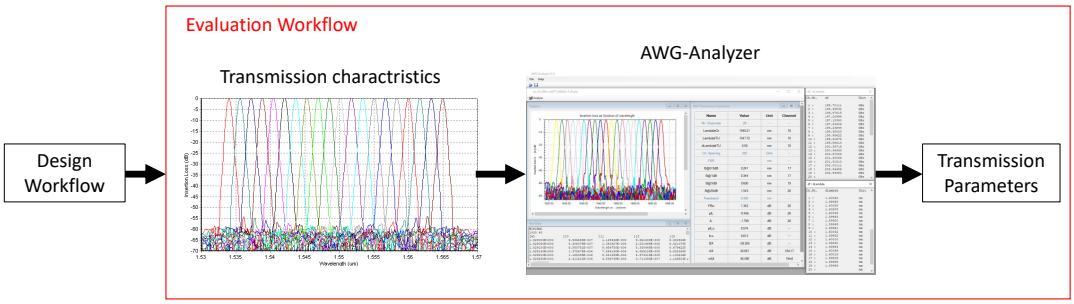

Figure 1.10: Evaluation Workflow of an AWG.

The AWG-Analyzer tool is an essential element for this work, therefore it will be described more in detail. Figure 1.11 shows the user interface of the AWG-Analyzer tool evaluating a 20-channel 200-GHz AWG. The input data utilised by the Phasar tool are displayed in the "Raw Data" window. By visualising the data, the transmission characteristics are obtained which are shown in the "Diagram" window. The transmission parameters calculated by the AWG-Analyzer tool are displayed in the "AWG Transmission Parameters" window. All transmission parameters with their definitions are described in detail in [14].

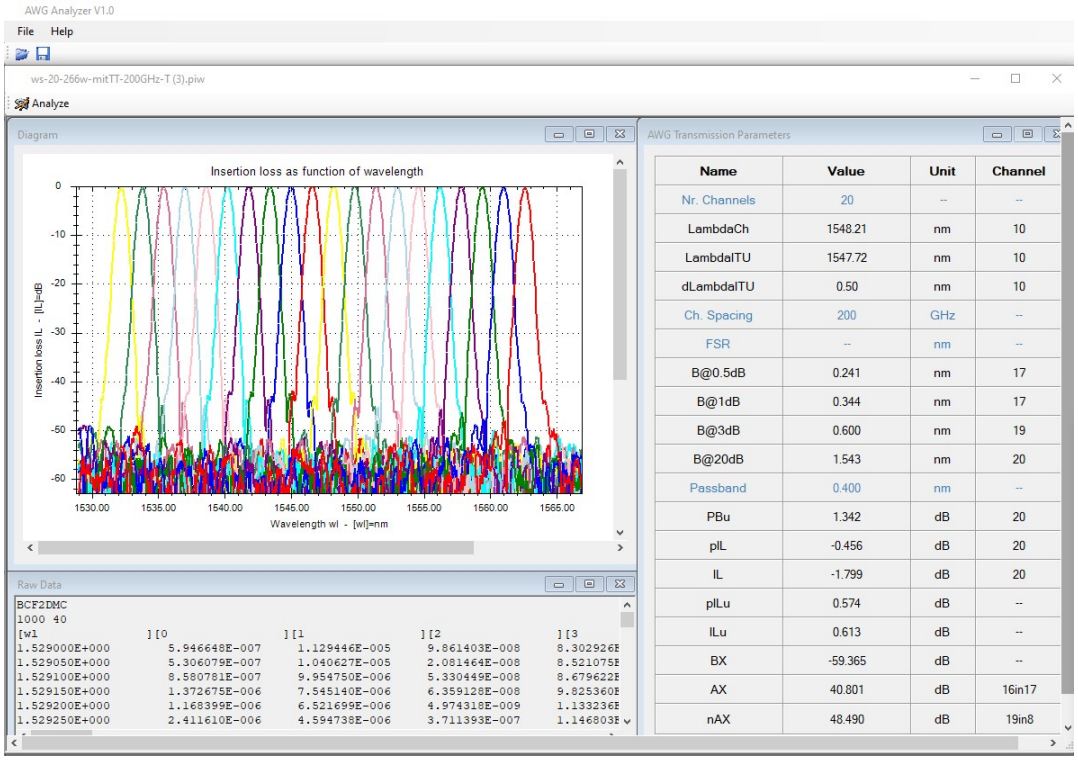

Figure 1.11: User interface of the AWG-Analyzer tool [14].

The transmission parameters which are important for this work are explained below.

Channel centre wavelength (λ_{cn})

The channel centre wavelength λ_{cn} is defined as the wavelength where a channel has the peak transmission (least insertion loss). Figure 1.12 illustrates the definition, where λ_{c4} is the channel centre wavelength of the fourth (violet) channel.

Channel Spacing in wavelength (dλ) and in frequency (df) domain

The channel spacing parameter $d\lambda$ is defined as the distance between the channel centre wavelengths of two adjacent transmission channels in the measured/simulated transmission characteristics, see Figure 1.12. The mathematical explanation is described by Equation 1.1, where i=[1;n-1] and n is the number of transmission channels.

$$d\lambda_i = |\lambda_{ci} - \lambda_{(ci+1)}| \tag{1.1}$$

To obtain the channel spacing in the frequency domain, Equation 1.2 is used, where c is the speed of light in the vacuum.

$$df_i = |\frac{\lambda_{ci}}{c} - \frac{\lambda_{(ci+1)}}{c}| \tag{1.2}$$

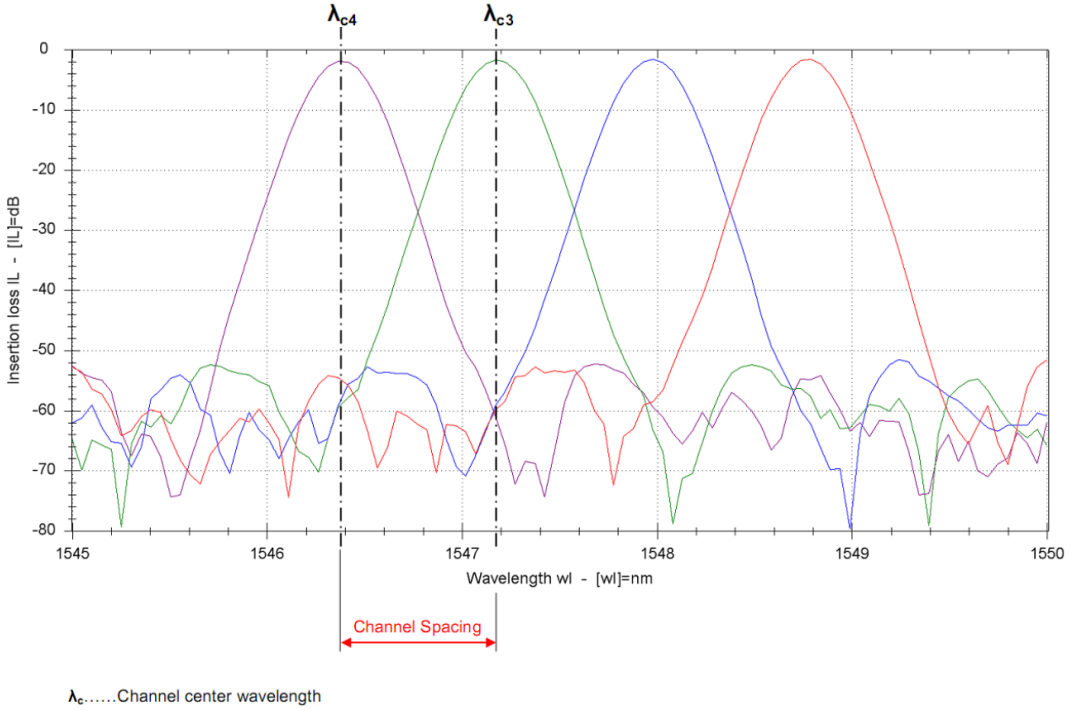

Figure 1.12: Channel spacing [14].

Peak Insertion loss (pIL)

The peak insertion loss is defined as the power loss from the 0 dB-line to the maximum of the transmission channel, as shown in Figure 1.13. The value indicates the worst of all channels.

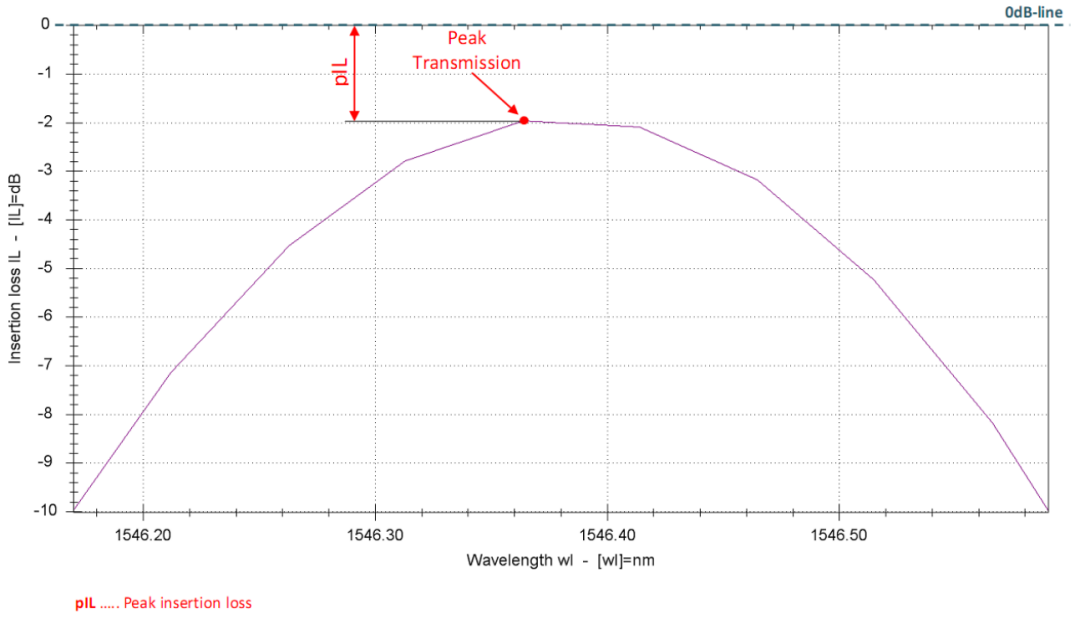

Figure 1.13: Peak insertion loss [14].

Insertion loss (IL)

The insertion loss is defined as the maximum loss within the passband from the 0 dB-line, as shown in Figure 1.14. It represents the worst value over all channels and considering both polarisation states.

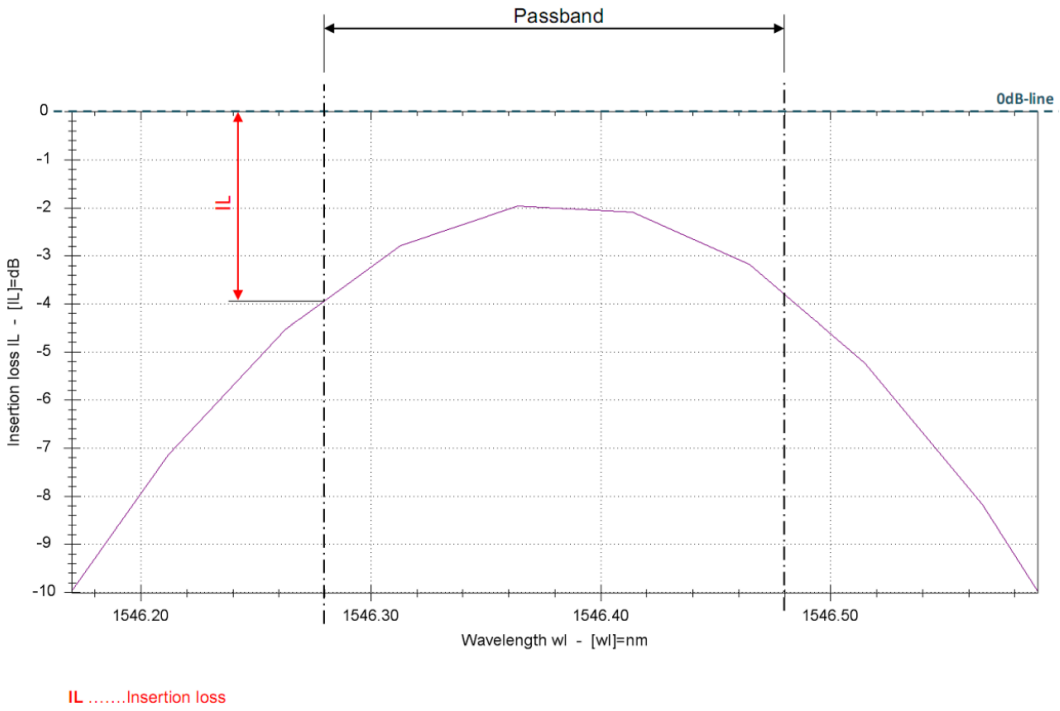

Figure 1.14: Insertion loss [14].

Insertion loss uniformity (ILu)

The insertion loss uniformity is defined as the difference between maximum and minimum insertion loss across all channels, as represented in Figure 1.15.

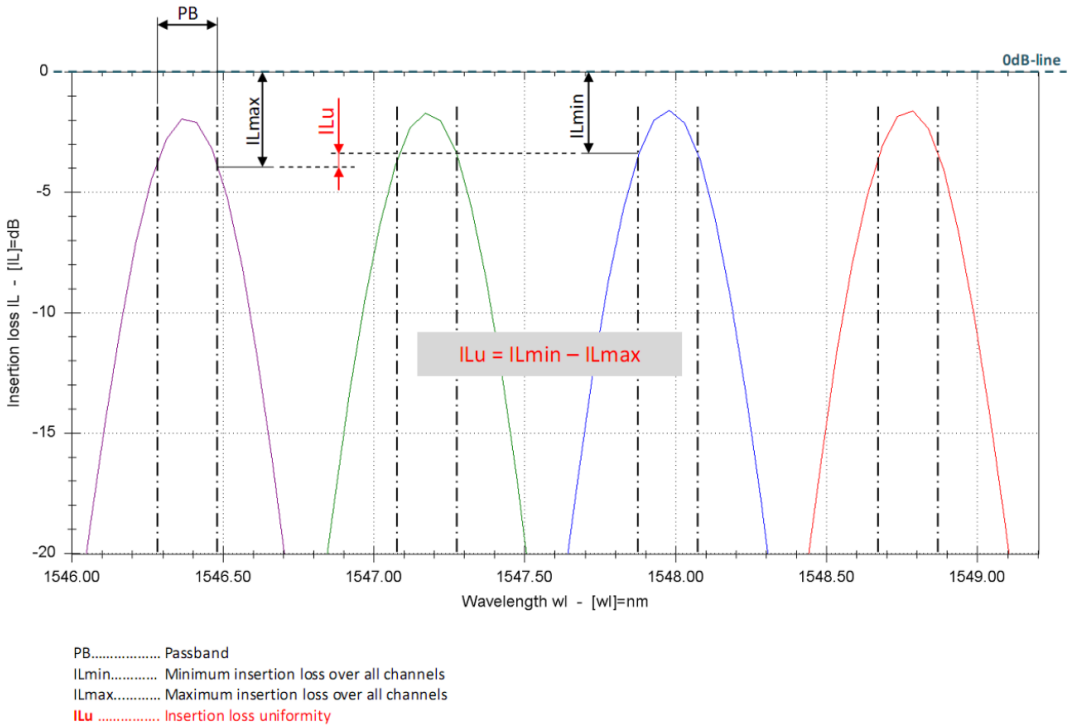

Figure 1.15: Insertion loss uniformity [14].

Peak insertion loss uniformity (pILu)

Peak insertion loss uniformity is defined as the difference of maximum and minimum peak insertion loss across all channels. The graphical representation of this parameter is illustrated in Figure 1.16.

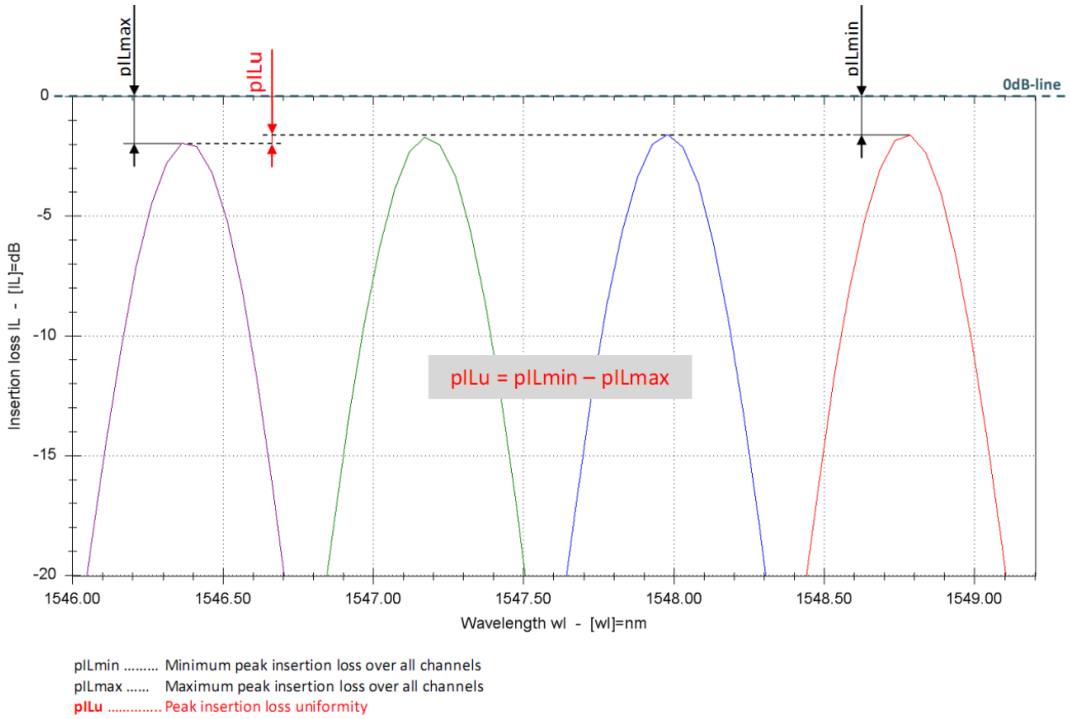

Figure 1.16: Peak insertion loss uniformity [14].

Adjacent channel crosstalk (AX)

Adjacent channel crosstalk is the unwanted power in the passband caused by the ad-jacent channel. The value describes the largest difference over all channels between the lowest transmission of the adjacent channel in the passband and the highest transmission. Figure 1.17 illustrates the definition of adjacent channel crosstalk.

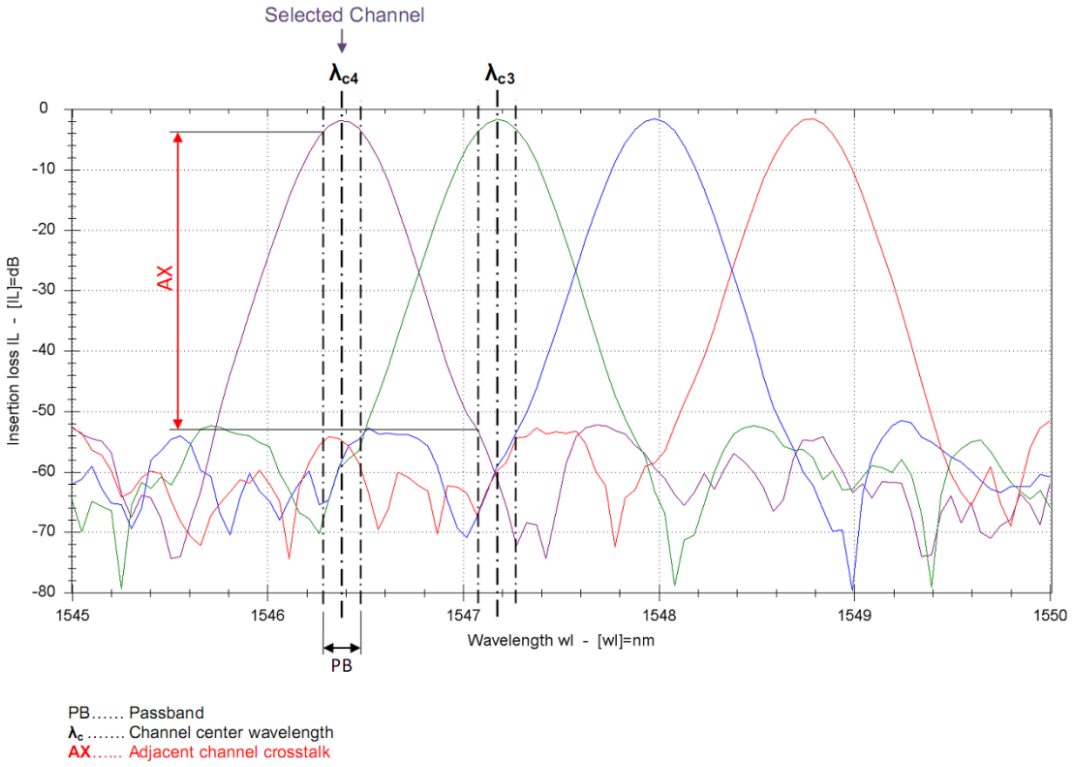

Figure 1.17: Adjacent channel crosstalk [14].

Non-adjacent channel crosstalk (nAX)

Non-adjacent channel crosstalk is the unwanted power in the passband caused by a non-adjacent channel. It is the worst-case difference between the lowest transmission in the passband of the selected channel and the highest transmission of the selected channel in the passband of any non-adjacent channel. The value indicates the worst case across all channels. Figure 1.18 shows the graphical representation of this definition.

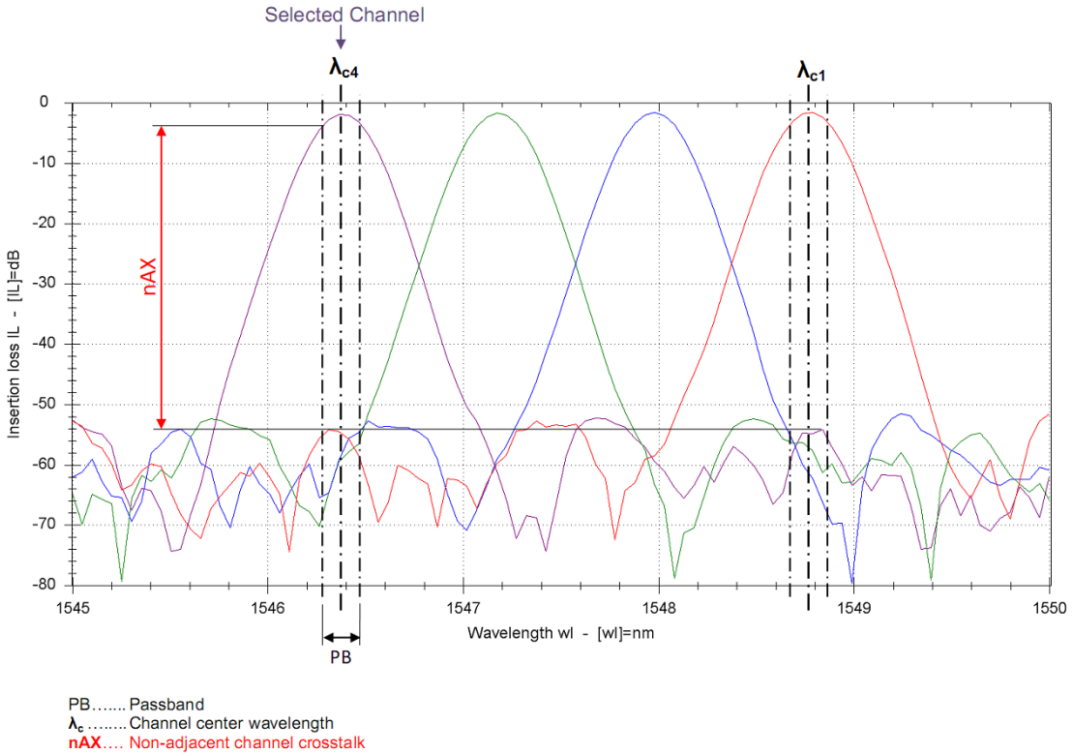

Figure 1.18: Non-adjacent channel crosstalk [14].

Background crosstalk (BX)

Background crosstalk is defined as the average peak transmission in the BX band of a channel. Where the BX band includes all wavelengths except the range of channel centre wavelength (+/- channel spacing). The value indicates the worst value for all channels. The graphical representation of the definition is shown in Figure 1.19.

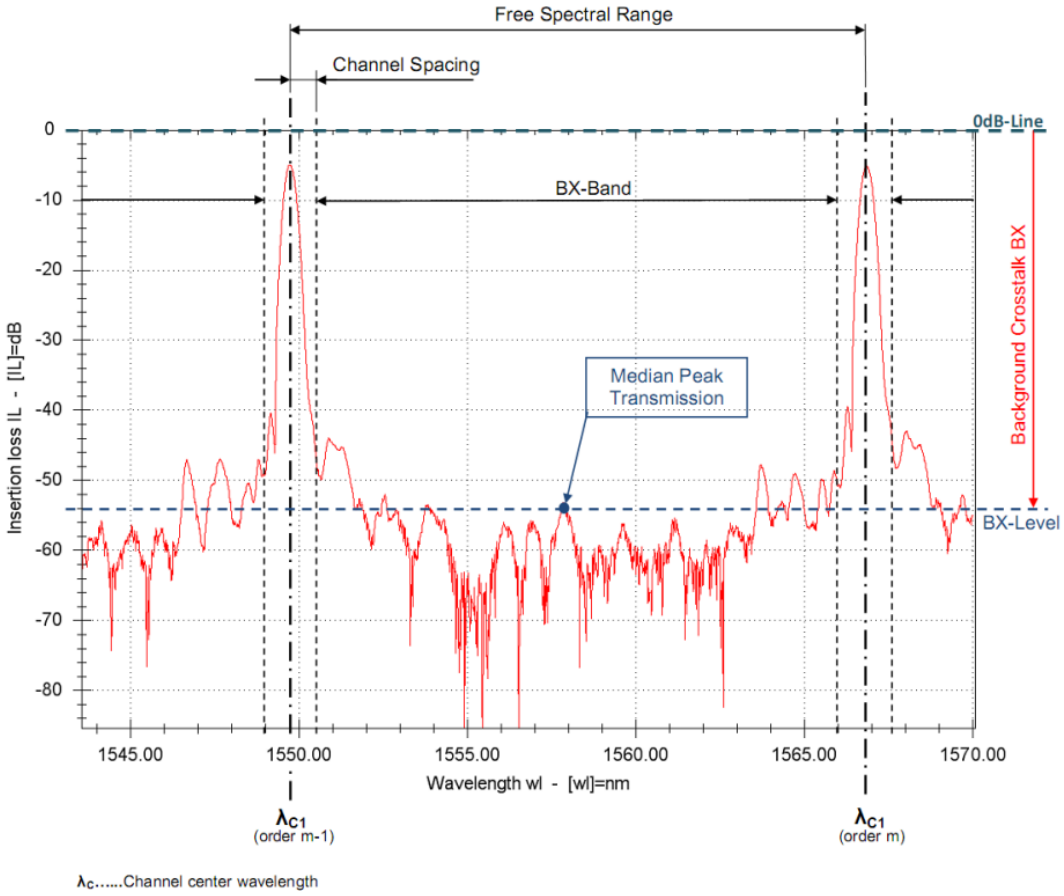

Figure 1.19: Background crosstalk [14].

1.1.5 ITU-Grid

The International Telecommunication Union (ITU) is the specialised agency of the United Nations in the field of telecommunications standardisation. The ITU organisation has developed recommendations on which central wavelengths or frequencies are particularly suitable for optical data transmission [15]. The resulting table is called the ITU-Grid. Figure 1.20 shows the ITU-Grid in the third operating window (L-Band, C-Band and S-Band). These central wavelengths or frequencies have the lowest power loss over long distances. The red rectangle represents the central frequencies with a channel spacing of 100 GHz, which is constant. The blue rectangle shows the central wavelengths, the channel spacing is about 0.8 nm (tending to decrease with channel number).

ITU Grid Specification

	L-Band				C-Band				S-Band			
	100 GHz Grid		50 GHz Offset		100 GHz Grid		50 GHz Offset		100 GHz Grid		50 GHz Offset	
	THz	nm	THz	nm	THz	nm	THz	nm	THz	nm	THz	nm
1	186.00	1611.79	186.05	1611.35	191.00	1569.59	191.05	1569.18	196.00	1529.55	196.05	1529.16
2	186.10	1610.92	186.15	1610.49	191.10	1568.77	191.15	1568.36	196.10	1528.77	196.15	1528.38
3	186.20	1610.06	186.25	1609.62	191.20	1567.95	191.25	1567.54	196.20	1527.99	196.25	1527.60
4	186.30	1609.19	186.35	1608.76	191.30	1567.13	191.35	1566.72	196.30	1527.22	196.35	1526.83
5	186.40	1608.33	186.45	1607.90	191.40	1566.31	191.45	1565.90	196.40	1526.44	196.45	1526.05
6	186.50	1607.47	186.55	1607.04	191.50	1565.50	191.55	1565.09	196.50	1525.66	196.55	1525.27
7	186.60	1606.60	186.65	1606.17	191.60	1564.68	191.65	1564.27	196.60	1524.89	196.65	1524.50
8	186.70	1605.74	186.75	1605.31	191.70	1563.86	191.75	1563.45	196.70	1524.11	196.75	1523.72
9	186.80	1604.88	186.85	1604.46	191.80	1563.05	191.85	1562.64	196.80	1523.34	196.85	1522.95
10	186.90	1604.03	186.95	1603.60	191.90	1562.23	191.95	1561.83	196.90	1522.56	196.95	1522.18
11	187.00	1603.17	187.05	1602.74	192.00	1561.42	192.05	1561.01	197.00	1521.79	197.05	1521.40
12	187.10	1602.31	187.15	1601.88	192.10	1560.61	192.15	1560.20	197.10	1521.02	197.15	1520.63
13	187.20	1601.46	187.25	1601.03	192.20	1559.79	192.25	1559.39	197.20	1520.25	197.25	1519.86
14	187.30	1600.60	187.35	1600.17	192.30	1558.98	192.35	1558.58	197.30	1519.48	197.35	1519.09
15	187.40	1599.75	187.45	1599.32	192.40	1558.17	192.45	1557.77	197.40	1518.71	197.45	1518.32
16	187.50	1598.89	187.55	1598.47	192.50	1557.36	192.55	1556.96	197.50	1517.94	197.55	1517.55
17	187.60	1598.04	187.65	1597.62	192.60	1556.55	192.65	1556.15	197.60	1517.17	197.65	1516.78
18	187.70	1597.19	187.75	1596.76	192.70	1555.75	192.75	1555.34	197.70	1516.40	197.75	1516.02
19	187.80	1596.34	187.85	1595.91	192.80	1554.94	192.85	1554.54	197.80	1515.63	197.85	1515.25
20	187.90	1595.49	187.95	1595.06	192.90	1554.13	192.95	1553.73	197.90	1514.87	197.95	1514.49
21	188.00	1594.64	188.05	1594.22	193.00	1553.33	193.05	1552.93	198.00	1514.10	198.05	1513.72
22	188.10	1593.79	188.15	1593.37	193.10	1552.52	193.15	1552.12	198.10	1513.34	198.15	1512.96
23	188.20	1592.95	188.25	1592.52	193.20	1551.72	193.25	1551.32	198.20	1512.58	198.25	1512.19
24	188.30	1592.10	188.35	1591.68	193.30	1550.92	193.35	1550.52	198.30	1511.81	198.35	1511.43
25	188.40	1591.26	188.45	1590.83	193.40	1550.12	193.45	1549.72	198.40	1511.05	198.45	1510.67
26	188.50	1590.41	188.55	1589.99	193.50	1549.32	193.55	1548.91	198.50	1510.29	198.55	1509.91
27	188.60	1589.57	188.65	1589.15	193.60	1548.51	193.65	1548.11	198.60	1509.53	198.65	1509.15
28	188.70	1588.73	188.75	1588.30	193.70	1547.72	193.75	1547.32	198.70	1508.77	198.75	1508.39
29	188.80	1587.88	188.85	1587.46	193.80	1546.92	193.85	1546.52	198.80	1508.01	198.85	1507.63
30	188.90	1587.04	188.95	1586.62	193.90	1546.12	193.95	1545.72	198.90	1507.25	198.95	1506.87
31	189.00	1586.20	189.05	1585.78	194.00	1545.32	194.05	1544.92	199.00	1506.49	199.05	1506.12
32	189.10	1585.36	189.15	1584.95	194.10	1544.53	194.15	1544.13	199.10	1505.74	199.15	1505.36
33	189.20	1584.53	189.25	1584.11	194.20	1543.73	194.25	1543.33	199.20	1504.98	199.25	1504.60
34	189.30	1583.69	189.35	1583.27	194.30	1542.94	194.35	1542.54	199.30	1504.23	199.35	1503.85
35	189.40	1582.85	189.45	1582.44	194.40	1542.14	194.45	1541.75	199.40	1503.47	199.45	1503.10
36	189.50	1582.02	189.55	1581.60	194.50	1541.35	194.55	1540.95	199.50	1502.72	199.55	1502.34
37	189.60	1581.18	189.65	1580.77	194.60	1540.56	194.65	1540.16	199.60	1501.97	199.65	1501.59
38	189.70	1580.35	189.75	1579.93	194.70	1539.77	194.75	1539.37	199.70	1501.21	199.75	1500.84
39	189.80	1579.52	189.85	1579.10	194.80	1538.98	194.85	1538.58	199.80	1500.46	199.85	1500.09
40	189.90	1578.69	189.95	1578.27	194.90	1538.19	194.95	1537.79	199.90	1499.71	199.95	1499.34
41	190.00	1577.86	190.05	1577.44	195.00	1537.40	195.05	1537.00	200.00	1498.96	200.05	1498.59
42	190.10	1577.03	190.15	1576.61	195.10	1536.61	195.15	1536.22	200.10	1498.21	200.15	1497.84
43	190.20	1576.20	190.25	1575.78	195.20	1535.82	195.25	1535.43	200.20	1497.46	200.25	1497.09
44	190.30	1575.37	190.35	1574.95	195.30	1535.04	195.35	1534.64	200.30	1496.72	200.35	1496.34
45	190.40	1574.54	190.45	1574.13	195.40	1534.25	195.45	1533.86	200.40	1495.97	200.45	1495.60
46	190.50	1573.71	190.55	1573.30	195.50	1533.47	195.55	1533.07	200.50	1495.22	200.55	1494.85
47	190.60	1572.89	190.65	1572.48	195.60	1532.68	195.65	1532.29	200.60	1494.48	200.65	1494.11
48	190.70	1572.06	190.75	1571.65	195.70	1531.90	195.75	1531.51	200.70	1493.73	200.75	1493.36
49	190.80	1571.24	190.85	1570.83	195.80	1531.12	195.85	1530.72	200.80	1492.99	200.85	1492.62
50	190.90	1570.42	190.95	1570.01	195.90	1530.33	195.95	1529.94	200.90	1492.25	200.95	1491.88

Figure 1.20: ITU-Grid [16].

1.2 Problem Description

Due to the frequency to wavelength dependency described by Equation 1.3, where c is the speed of light, it is not possible to have a constant channel spacing in the frequency and wavelength domain at the same time.

$$f(\lambda) = \frac{c}{\lambda} \tag{1.3}$$

Figure 1.21 shows the Equation 1.3 graphically, as can be seen the wavelength to frequency dependence is not linear. Consequently, the channel spacing can be constant either in the wavelength domain or in the frequency domain.

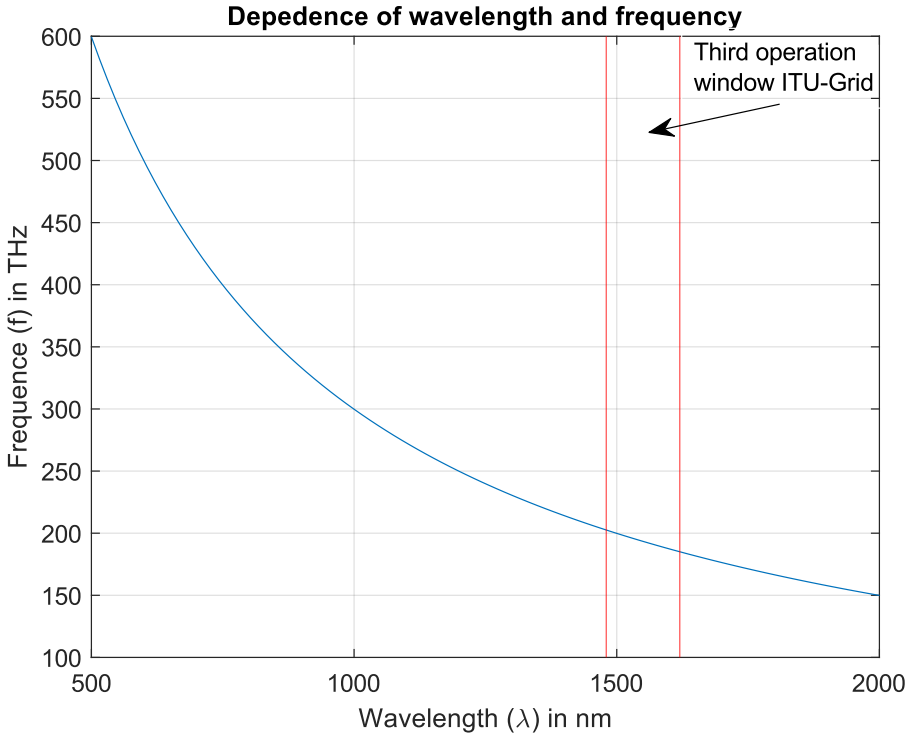

Figure 1.21: Depedence of wavelenght and frequency.

Based on the evaluation process described in Subsection 1.1.4.3, the following channel spacing is obtained for a simulated 20-channel 200-GHz AWG, which is shown graphically in Figure 1.22. The left graph illustrates the channel spacing in the wavelength domain, where the value is constant at 1.6 nm. The channel spacing in the frequency domain, which is shown in the graph on the right, is not constant. It decreases from about 203 GHz to about 196 GHz with increasing channel number (Num).

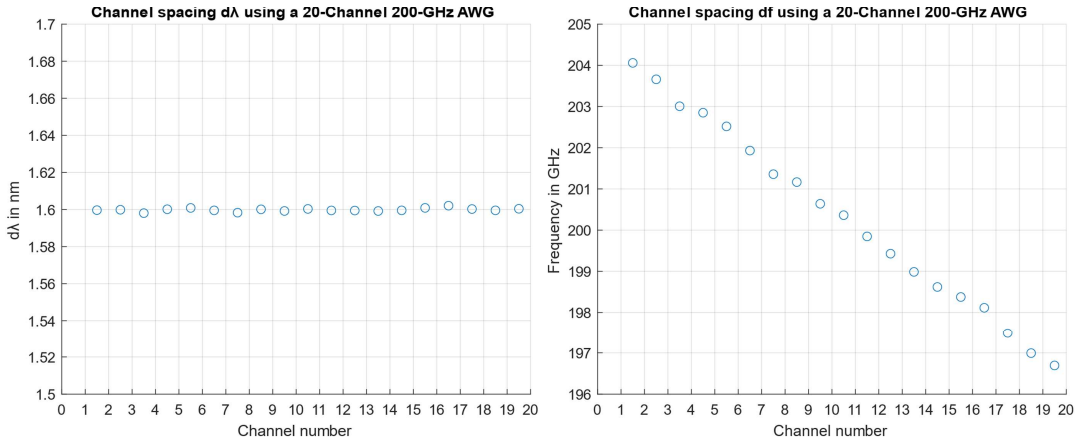

Figure 1.22: Simulated channel spacing in wavelength and frequency domain.

The measured channel spacing of a 20-channel 200-GHz AWG is shown in Figure 1.23, which shows the same tendency of the channel spacing. The deviation from linearity is because the refraction index does not exactly match with the simulated one.

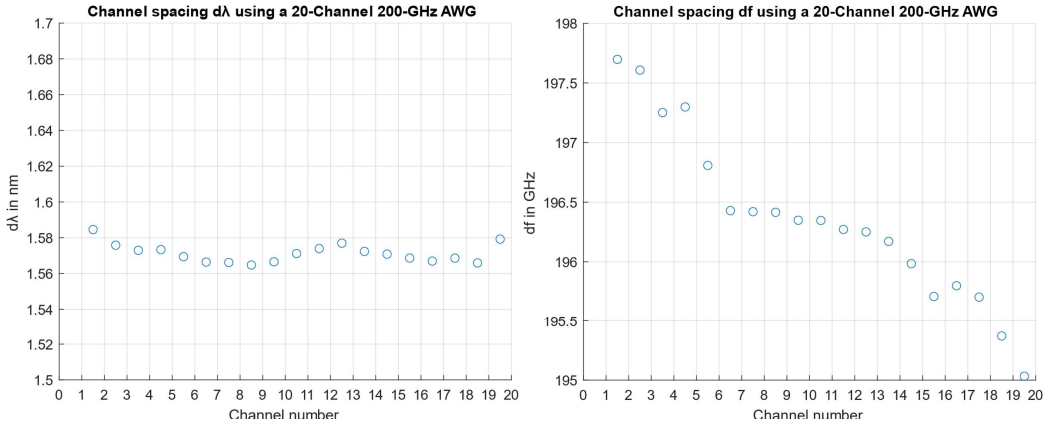

Figure 1.23: Measured channel spacing in wavelength and frequency domain.

According to the ITU-Grid described in the previous section, the channel spacing for telecommunication applications should be constant in the frequency domain. This nonconformity with the ITU-Grid can lead to data loss, as the photodetectors on the receiver side are designed to detect optical signals that conform to the ITU-Grid.

In summary, the problem is that the design process of an AWG results in the channel spacing being constant in the wavelength domain. According to the ITU-Grid, the channel spacing should be constant in the frequency domain. This mismatch can lead to data loss in modern fibre optic networks.

1.3 Objectives

The main objective of this thesis is to develop a tool that corrects (optimises) the channel spacing of an AWG so that it corresponds to the ITU-Grid. For the correction, several methods were developed at the Vorarlberg University of Applied Sciences. These will be described and compared with each other to determine which method achieves the best results. In addition, the transmission parameters of the original design will be compared with the optimised design.

The objectives of this work are:

- Introduction to the theory of optical data transmission and optical MUX/ DEMUX based on arrayed waveguide gratings.
- Development of a new tool to maintain channel spacing according to the ITU-Grid. The tool has the following requirements:
  - User friendly
  - Standalone executable program (no need of other programs to start the tool)
  - Visualise of the data
  - Saving of the data
- Verify the tool with different designed AWGs.
- Compare the results of the different developed methods.
- Compare the transmission parameters before and after the optimisation.

2 Methodology

This section describes the concept of how to solve the problem explained in Section 1.2. Furthermore, the different methods developed at the Vorarlberg University of Applied Sciences and the optimisation workflow are described.

2.1 Concept to Solve the Problem

As can be seen in Figure 2.1, all transmission signals (wavelengths) are focused each at one well-defined point lying on the focal line in the output coupler. All these points have a constant distance i.e. the channel spacing, $d\lambda$ between the wavelengths λ_1-λ_n is also constant. It follows that the positions of the output waveguides, given by the parameter dx, are also constant. By shifting the positions of the output waveguides, i.e. by recalculating the parameter dx, the parameter channel spacing, df can be corrected very precisely to a constant value.

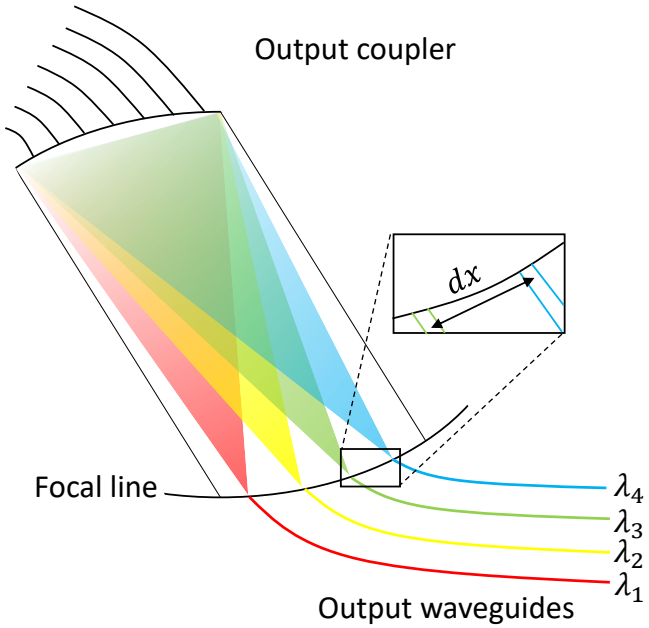

Figure 2.1: Output coupler of an AWG.

There are three methods to adjust the parameter dx which were developed at the Vorarlberg University of Applied Sciences:

- Proportional method [17]
- Angular method [18]
- Position method [19]

2.1.1 Proportional method

The proportional method calculates from a set of three parameters

- designed channel spacing, df
- designed output waveguide separation, dx
- calculated channel spacing, df_n

the corrected output waveguide separation parameter, df_n to obtain the desired channel spacing, df. As already mentioned, the designed parameter dx is constant (in Figure 2.2 dx with the blue arrow). Using the proportional method results in Num - 1 dx_n-values (where Num is the number of output channels) which are no longer constant (in Figure 2.2 dx_n with the red arrows).

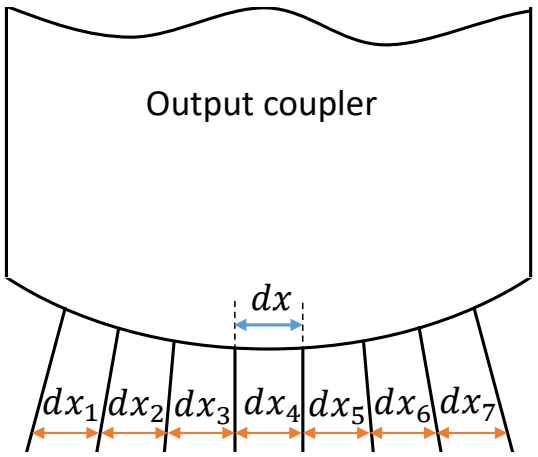

Figure 2.2: Proportional method.

Equation 2.1 shows the mathematical description of this calculation:

$$dx_n = \frac{dx * df}{df_n} \tag{2.1}$$

2.1.2 Angular method

For optimisation with the angular method, the parameters used for the proportional method and additionally *Lf* (length of the coupler) are required. To maintain the desired channel spacing *df*, the first step is to calculate the angle (α) between the constant *dx*, see Figure 2.3.

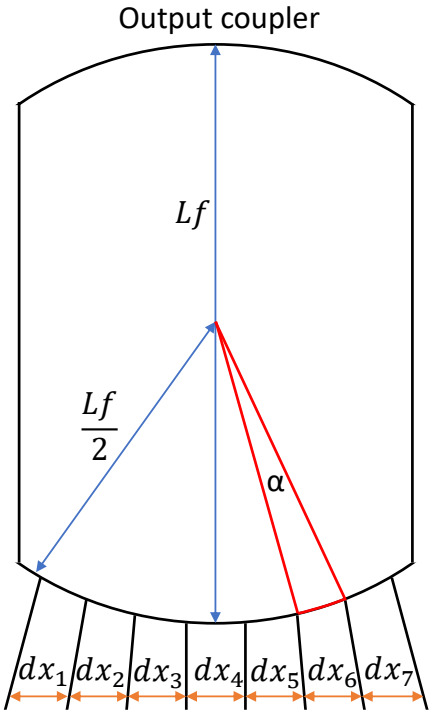

Figure 2.3: Angular method.

The calculation is carried out using the isosceles triangle formula described by Equation 2.2 and the result is in radians.

$$\alpha = 2 * arcsin(\frac{dx}{df}) = dx^{\circ} \tag{2.2}$$

Equation 2.3 calculates the new $dx_n{}^{\circ}$ values in radians.

$$dx_n{}^{\circ} = \frac{dx^{\circ} * df}{df_n} \tag{2.3}$$

To obtain the values in a unit of length (μm), equation 2.4 is used. Applying this method results in *Num - 1* dx_n values for dx_n.

$$dx_n = \frac{Lf}{2 * dx_n{}^{\circ}} \tag{2.4}$$

2.1.3 Position Method

To achieve the desired channel spacing *df* with the position method, the same parameters used for the proportional method are required. The principle of this method is to determine the positions that correspond to the desired channel spacing *df*. The schematic concept of the position method is illustrated in Figure 2.4.

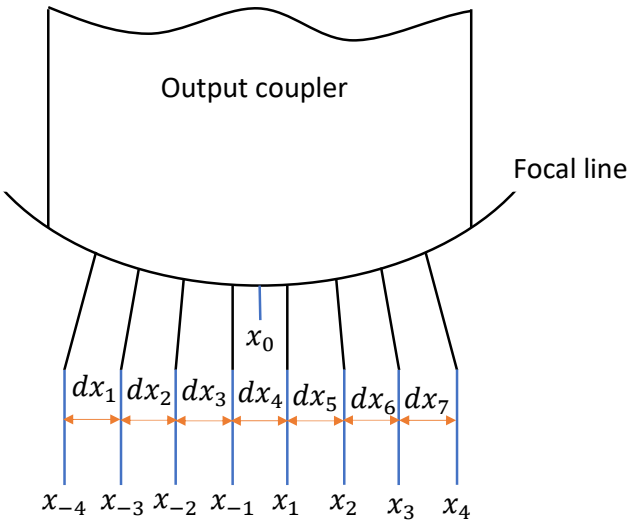

Figure 2.4: Position method.

As shown in Figure 2.4, the transmission channels $\lambda_1, \ldots, \lambda_n$ focus symmetrically on the focal line around the null position x_0. Equation 2.5 calculates the new positions $x_{-\frac{Num}{2}}), \ldots, \ x_{-1)}$ of the focused transmission channels $(\lambda_1, \ldots, \lambda_{\frac{Num}{2}}$ on the left side.

$$x_{-k} = \frac{(\frac{dx}{2} + (|k| - 1) * dx) * (\frac{df}{2} + (|k| - 1) * df}{\frac{df_{\frac{Num}{2}}}{2} + \sum_{i=\frac{Num}{2}-(|k|-1)}^{i=\frac{Num}{2}-1} df_i} \tag{2.5}$$

The new positions of x_1 and x_2 are calculated as shown in Equation 2.6.

$$x_1 = x_{-1} = \frac{dx * df}{2 * df_{\frac{Num}{2}}} \tag{2.6}$$

To calculate the new positions $(x_1, \ldots, x_{\_\frac{Num}{2}})$ of the focused transmission channels $(\lambda_{\frac{Num}{2}+1}, \ldots, \lambda_{Num})$ on the right side, Equation 2.7 is used.

$$x_k = \frac{(\frac{dx}{2} + (k-1) * dx) * (\frac{df}{2} + (k-1) * df}{\frac{df_{\frac{Num}{2}}}{2} + \sum_{i=\frac{Num}{2}+1}^{i=\frac{Num}{2}+(k-1)} df_i} \tag{2.7}$$

To determine the dx_n-values, the differences of the positions are calculated as follows:

- For the left side: $dx_n = x_{-k} - x_{-k+1}$
  where $k = [1, \frac{Num}{2}]$ and $n = [1, \frac{Num}{2} - 1]$
- For the center: $dx_{\frac{Num}{2}-1} = x_1 + x_{-1}$
- For the right side: $dx_n = x_k - x_{k+1}$
  where $k = [\frac{Num}{2}, Num]$ and $n = [\frac{Num}{2} + 1, \frac{Num}{2} - 1]$

2.2 Optimisation of the Methods

The previously mentioned methods for calculating the dx_n-values were evaluated with a 20-channel 200-GHz AWG. Figure 2.5 shows the resulting dx_n-values of the 20-channel 200-GHz AWG calculated with the mean of the dx_n-values of the proportional, angular and position methods in red ("dx_n over average of proportional, angular and position method"). It is obvious that the trend is linearly increasing, but errors in linearity occur. The reason for these errors is due to the fact that Phasar performs the simulation of the transmission characteristics in the discrete frequency range. These discrete values for the transmission characteristics are not corrected in the AWG-Analyzer tool, resulting in an error in the central wadvelengths required for the dx_n-values. The concept of correcting these errors is to find a linear function (regression line) that is the best possible approximation to the average of the dx_n-values. For the fitting of the regression lines, the least squares approximation is applied. The least squares approach is to determine the regression line that minimises the errors across all transmission channels. The regression line has the form of a linear function which can be seen in Equation 2.8. The y variable corresponds to the average dx_n-values calculated by the methods explained above and the x variable corresponds to the channel number [20].

$$y(x) = m * x + c \tag{2.8}$$

The least squares approximation is used to calculate the slope of the regression, see Equation 2.9. The variables $\overline{y}$ and $\overline{x}$ are the average and n is the number of values.

$$m = \frac{\sum_{i=1}^{n}(x_i - \overline{x}) * (y_i - \overline{y})}{\sum_{i=1}^{n}(x_i - \overline{x})^2} \tag{2.9}$$

The displacement constant c is calculated with Equation 2.10.

$$c = \overline{y} - m * \overline{x} \tag{2.10}$$

Figure 2.5 shows the calculated regression line of the 20-channel 200-GHz AWG "Regression line" and the corresponding "dx_n-values over regression method".

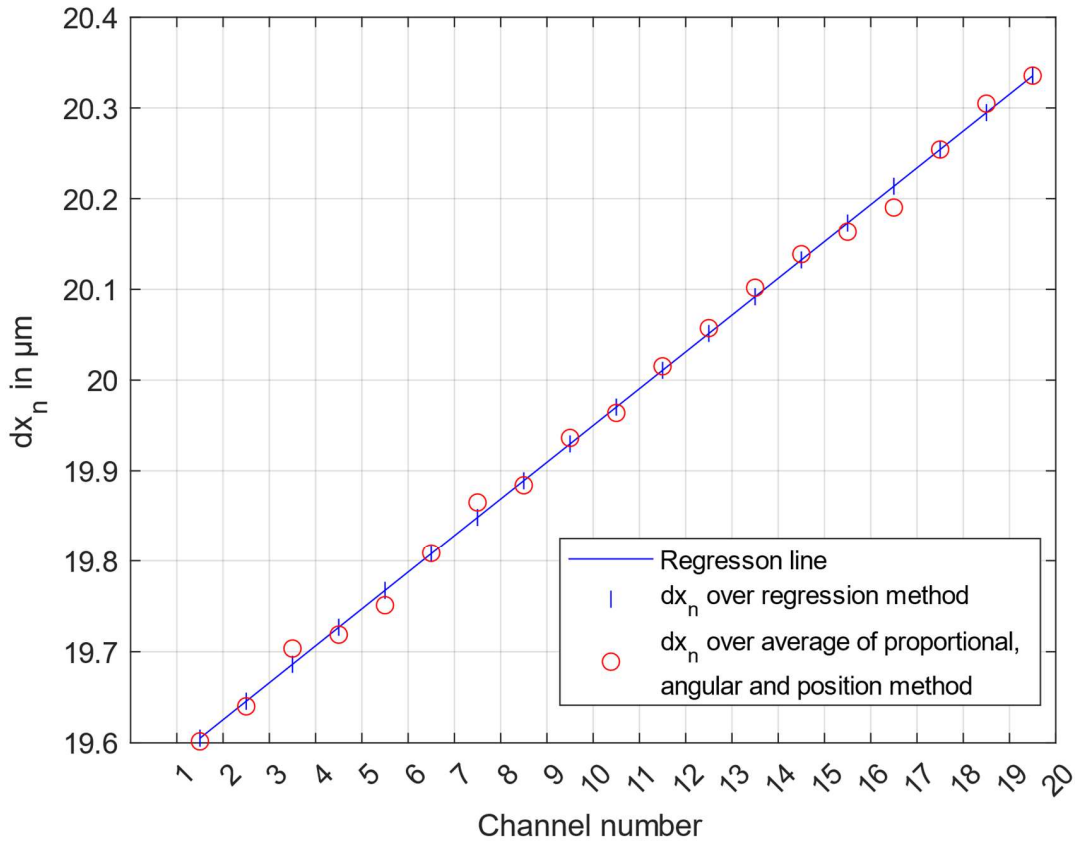

Figure 2.5: Concept for the optimisation of the methods.

The resulting channel spacing df in the frequency domain of the dx_n-values over the regression line are shown in Figure 2.6.

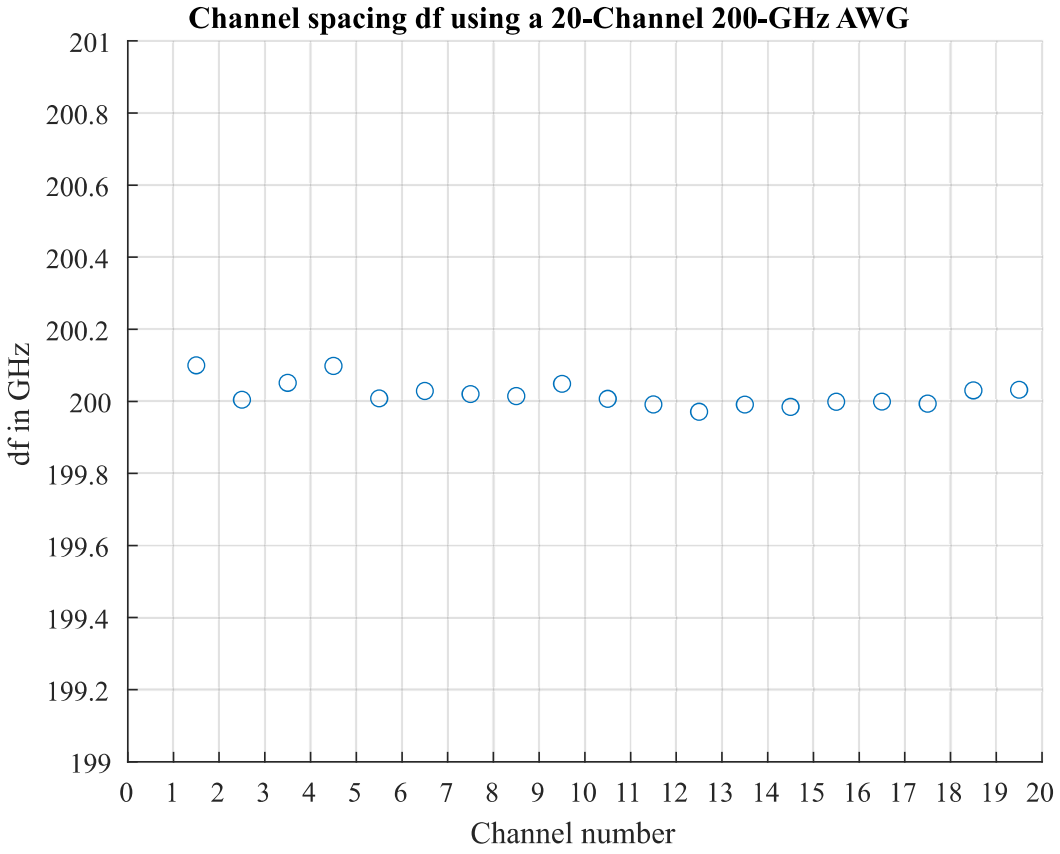

Figure 2.6: Concept for the optimisation of the methods.

This approach provides quite accurately the required constant channel spacing in the frequency domain. Additionally, another concept is developed, which provides similar results. In this concept, the average of the dx_n-values over the methods is subtracted from the dx_n-values over the regression method. A treshhold of 10 nm is applied and the correction of the dx_n-values is performed as follows:

- If $|dx_{n,average} - dx_{n,regression}| \leq 10\ nm$ then set $dx_n = dx_{n,average}$
- If $|dx_{n,average} - dx_{n,regression}| > 10\ nm$ then set $dx_n = \frac{dx_{n,average} + dx_{n,regression}}{2}$

2.3 Optimisation Workflow of an AWG

This section explains how the previously described methods are integrated into the development process of an AWG and the concept of the optimisation workflow. Figure 2.7 illustrates the entire development process of an AWG, divided into design, evaluation and optimisation workflow.

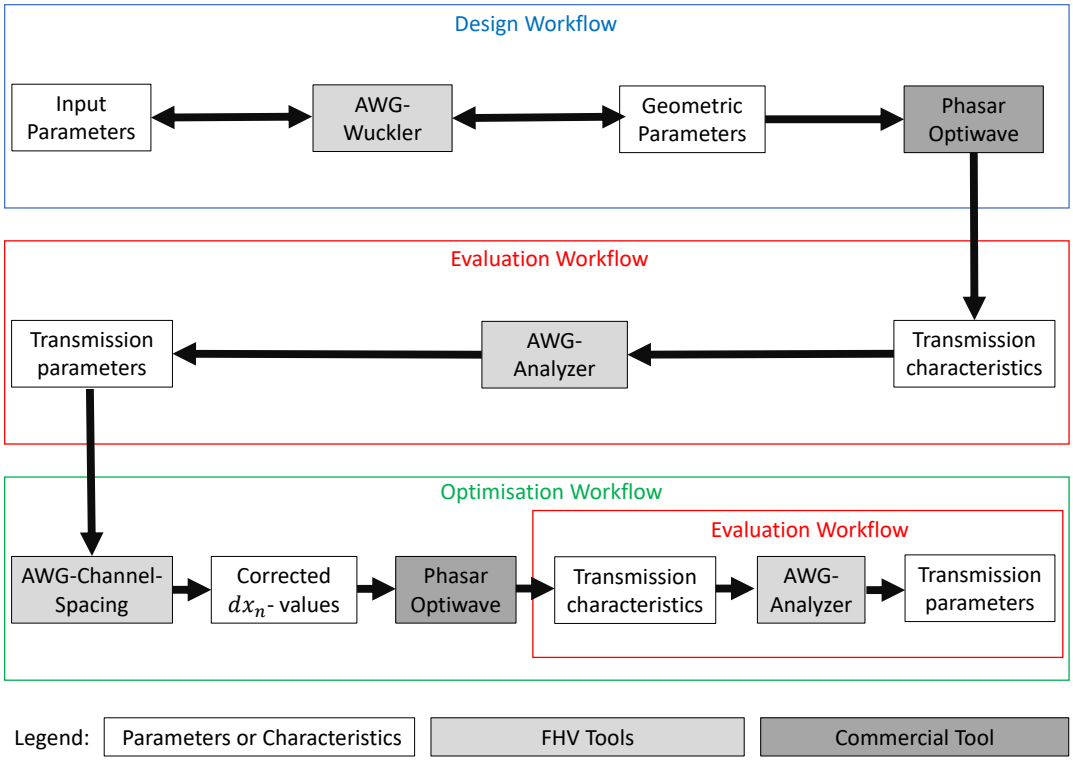

Figure 2.7: User interface AWG-Channel-Spacing.

For AWG used for telecommunication applications, the optimisation workflow is required to maintain the channel spacing according to the ITU-Grid. The AWG-Channel-Spacing tool developed in this work calculates the new dx_n-values using the methods described in Subsection 2.1.1 - 2.1.3. The geometric parameters dx, df and Lf are used as input for the AWG-Channel-Spacing tool. Additionally, the channel central wavelengths (λ_{cn}) calculated by the AWG-Analyzer tool are required. The AWG-Channel-Spacing tool converts these central wavelengths to central frequencies, f_{cn}. From them, the channel spacing in the frequency domain (df) is calculated, since these values are required for the methods. Using the Phasar Optiwave tool, the AWG is redesigned and re-simulated with the new dx_n-values. The AWG is re-evaluated to validate the performance of the AWG and to ensure that the channel spacing is correct according to the ITU-Grid.

3 AWG-Channel-Spacing Tool

This section describes the AWG-Channel-Spacing tool developed in this thesis. Specifically, the structure of the AWG-Channel-Spacing tool and its functions are illustrated using a flowchart. The Unified Modelling Language (UML) diagram is used to illustrate the software architecture of the tool. The next section describes the software environment utilised for the AWG-Channel-Spacing tool.

3.1 Software Environment

The AWG-Channel-Spacing tool is developed for use on the Windows operating system and is written in C++. This programming language supports object-oriented programming. The idea of object-oriented programming is to approximate the usually abstract world of software development to the real world. The tool is developed with the application framework and Graphical User Interface (GUI) toolkit QT [21]. The concept of QT are signals and slots that are used for communication between different objects. The advantage over other GUI toolkits is that QT automatically disconnects when one of the two communicating objects is deleted. This prevents the program from crashing and simplifies it [22, 23]. In addition, QT provides a detailed and supportive documentation. For these reasons, this framework was chosen for this work.

3.2 Concept of the AWG-Channel-Spacing Tool

The concept of the AWG-Channel-Spacing tool is shown in Figure 3.1 in form of a flow chart. The input parameters for the AWG-Channel-Spacing tool consist of the channel centre wavelengths ($\lambda_{c1} \ldots \lambda_{cn}$), the channel number ($Num$), and the geometric parameters (designed dx, designed df and Lf). The channel centre wavelengths are obtained from the AWG-Analyzer tool, while the other parameters originate from the AWG-Wuckler tool. The input parameters are verified for possible errors before the calculation. If the program detects a possible error, a warning is displayed, and the calculation will not start. If the input parameters are correct, the dx_n-values are calculated using the methods described in Subsection 2.1.1 - 2.1.3. These dx_n-values are also recalculated using the adjustment described in Section 2.2. These dx_n-values can be displayed

either in the form of a table or graphically. In addition, the parameters required for the calculation such as channel centre frequency (f_{cn}), channel spacing in the frequency (df) and wavelength domain ($d\lambda$) are also displayed in the table or in the graphical view. To import the dx_n-values into the Phasar tool, the values are saved in a dat (data) file. This requires the selection of the desired calculation method used to calculate dx_n-values. The individual steps and the user interface of the AWG-Channel-Spacing tool are explained in more detail in the following subsections.

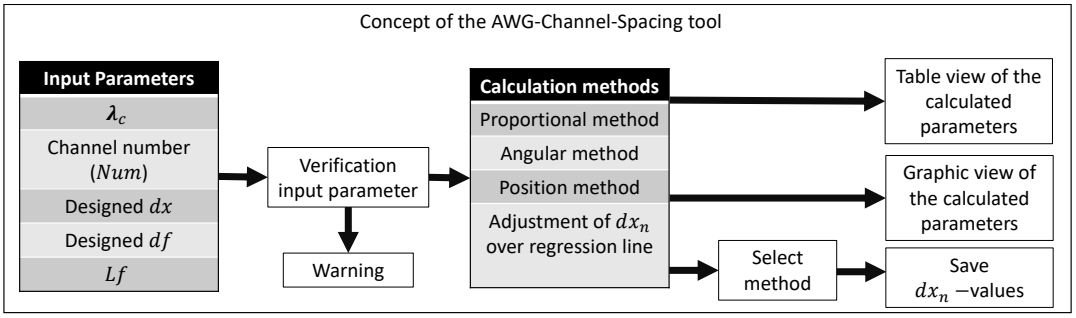

Figure 3.1: Concept of the AWG-Channel-Spacing tool.

3.3 User Interface

The graphical user interface of the AWG-Channel-Spacing tool is shown in Figure 3.2. It is based on the main window in which all functions are executed. It consists of several sub-windows. The “Channel Centre Wavelength (Original)” window is used to import the channel centre wavelengths ($\lambda_{c1} \ldots \lambda_{cn}$) from the AWG-Analyzer tool. In addition, there are four input parameters: ”Channel Number (Num)”, ”Designed dx”, ”Designed df and Lf”. The ”Table View” button displays the calculated parameters in a table as described before, see ”Table View of the Calculated Parameters”. A graphical representation of the calculated parameters is obtained via the ”Graphics” button. Additionally, the optimised channel centre wavelength can be imported into the ”Channel Centre Wavelength (Optimised)” window. This allows the channel spacings in the frequency and wavelength domain of the original and the optimised AWG to be displayed and compared in a graph. To save the dx_n-values, the ”Save” button is used. In general, all three buttons are completely independent on each other. By moving the mouse over a button or input field, the colour of the background changes to clarify for the user what can be clicked or changed.

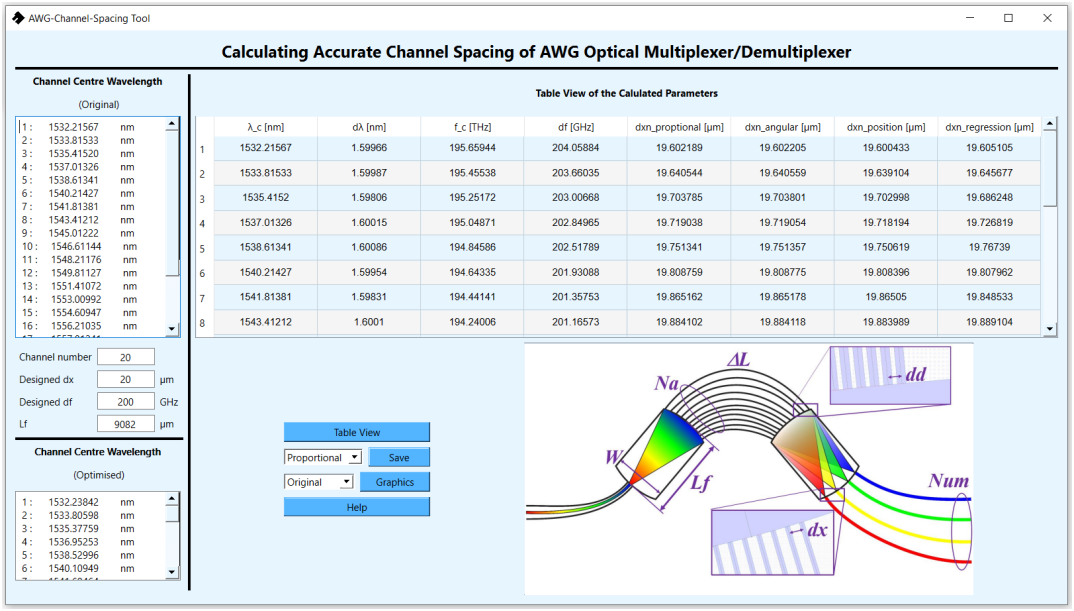

Figure 3.2: User interface AWG-Channel-Spacing.

3.4 Input Parameter

The input parameters "Channel Number (Num)", "Designed dx", "Designed df and Lf" are all individually typed in. As it would require more effort to enter all channel centre wavelengths individually, they can simply be copied from the AWG-Analyzer tool and pasted into the AWG-Channel-Spacing tool. These channel centre wavelengths from the AWG-Analyzer tool have all the pattern shown in Figure 3.3, which is from a 20-channel 200-GHz AWG.

```
1 :      1532.21567        nm
2 :      1533.81533        nm
3 :      1535.41520        nm
4 :      1537.01326        nm
5 :      1538.61341        nm
6 :      1540.21427        nm
7 :      1541.81381        nm
8 :      1543.41212        nm
9 :      1545.01222        nm
10 :     1546.61144        nm
11 :     1548.21176        nm
12 :     1549.81127        nm
13 :     1551.41072        nm
14 :     1553.00992        nm
15 :     1554.60947        nm
16 :     1556.21035        nm
17 :     1557.81241        nm
18 :     1559.41268        nm
19 :     1561.01223        nm
20 :     1562.61263        nm
```

Figure 3.3: Central wavelengths pattern from AWG-Analyzer tool.

This means that the channel number and the unit nm need to be extracted to obtain the channel central wavelengths. This is done by ignoring the first 10 characters and then extracting and storing the first channel central wavelength with 10 characters. Then all the central wavelengths can be extracted equally by ignoring 21 characters and then storing 10 characters as the next central wavelength. The pseudo code for this extraction is shown below. The obtained central wavelengths are stored in an array.

```
i = 10;

for(int Nr = 0; Nr < ChannelNumber; Nr++) {

  double Channel_center_wavelength[Nr] = store(i,store10).toDouble();

        i =i+31;  }
```

3.5 Functions

As described before, the AWG-Channel-Spacing tool provides the functions of displaying the parameters in a table, graphing the parameters, and saving the dx_n-values.
When executing one of these functions, the input parameters will be checked for possible errors first. If a possible error is detected, the warning window, shown in Figure 3.4 is displayed and the calculation will not start. The following causes a warning:

- Parameter is zero
- Parameter is empty
- Parameter is negative

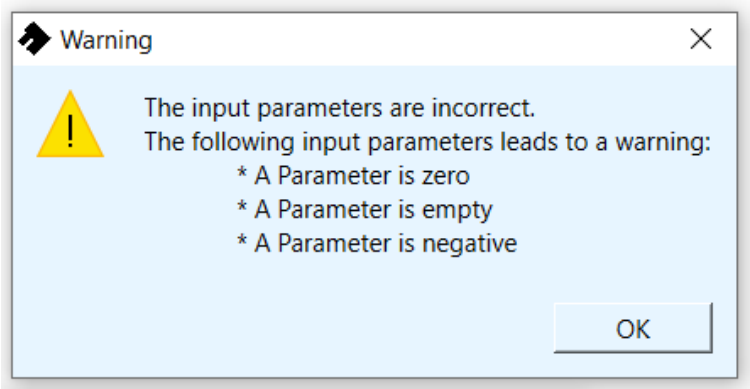

Figure 3.4: Warning window.

3.5.1 Table View

The "Table View" button creates a table in which the following parameters are calculated and displayed:

- Channel centre wavelengths in nm
- Channel spacing in the wavelength domain in nm
- Frequencies in THz
- Channel spacing in the frequency domain in GHz

- dx_n over the proportional method
- dx_n over the angular method
- dx_nover the position method
- dx_n over the regression line

In QT, table views are implemented with the model-based QTableView widget. With QTableView it is possible to display elements from a model. The model acts as an interface between QTableView and the data. The model contains the entries of the data and their indices. Regarding the AWG-Channel-Spacing tool, the upper parameters are stored in a matrix. To visualise the parameters in a table, the matrix is converted into a model and visualised with QTableView. The resulting table with the calculated parameters can be seen in Figure 3.2 under ” Table View of the Calculated Parameters”.

3.5.2 Graphics

The ”Graphics” button opens a new window in which the calculated parameters are displayed graphically, as shown in Figure 3.5.

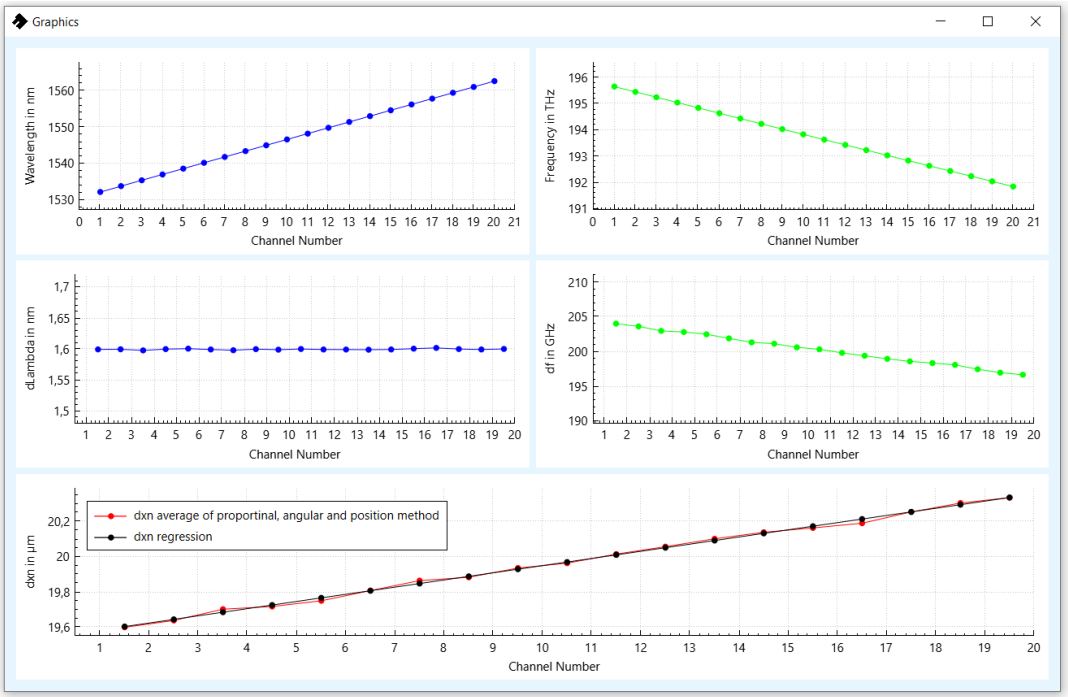

Figure 3.5: Charts.

This figure illustrates the parameters of the original 20-channel 200-GHz AWG. The upper diagrams show the central wavelengths (left diagram, "Wavelength [nm]") and the corresponding frequencies (right diagram, "Frequency [THz]"). The channel spacings in the frequency domain df and in the wavelength domain $d\lambda$ are shown in the middle diagrams. The average of the calculated dx_n-values over the methods and the adjusted dx_n-values are shown in the lower diagram. The axes of the diagrams are automatically adjusted. The highest and lowest values of the diagram are determined, and the Y-axis is adjusted to be slightly larger and smaller than these values.

The diagrams are created using the Qt C++ widget QCustomPlot [21], an open-source library for plotting and visualising data.

As mentioned in Section 3.3, it is also possible to display the parameters of the optimised AWG in the diagrams. This requires the channel centre wavelengths of the optimised AWG to be imported into the "Channel Centre Wavelength (Optimised)" window, see Figure 3.2. With the combo box, which is shown in Figure 3.6, the user can select whether the original, the optimised or both (see Figure 4.2) will be graphically displayed.

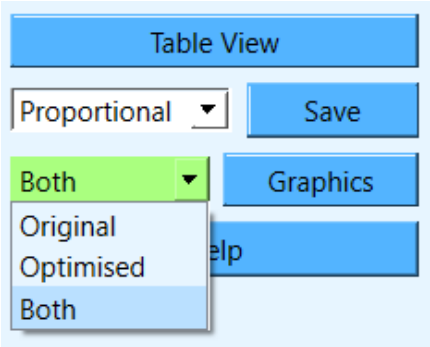

Figure 3.6: Combo box for graphical representation from original and optimised AWG.

3.5.3 Save

For inserting the calculated dx_n-values into the Phasar tool, they have to be saved in a dat-file first. The AWG-Channel-Spacing tool offers the possibility to select which calculation method (proportional, angular, position and adjusted over the regression line) should be saved for calculating the dx_n-values. The selection can be made via the combo box shown in Figure 3.2 (next to the "Save" button).

To import this dat-file into the Phasar tool, open the "WDM Device Properties" window and set the "Min. Wg. Separation" to individual, see Figure 3.7. The "Edit Separation" button opens the "Edit Waveguide Separation" window. The dat-file from the AWG-Channel-Spacing tool can simply be inserted with the "Load" button.

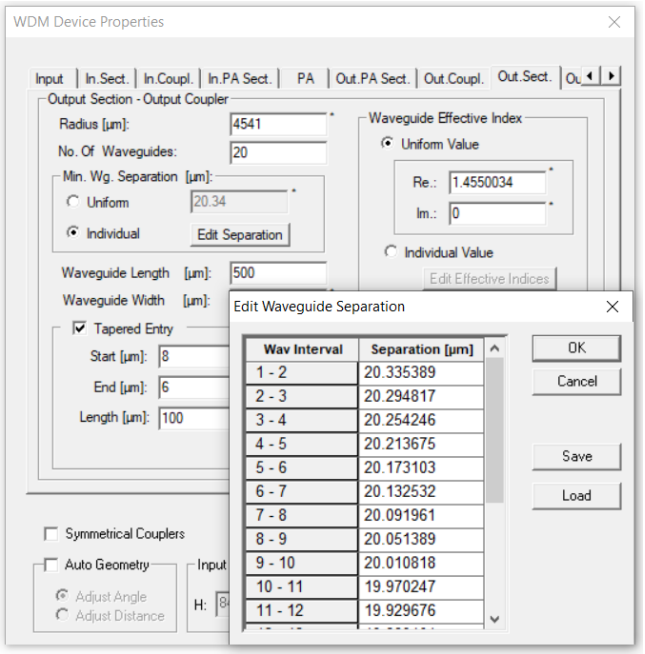

Figure 3.7: Insertion of dat-file in the Phasar tool

3.6 UML

To graphically illustrate the architecture of the AWG-Channel-Spacing tool, the class diagram of the tool is shown in Figure 3.8. A class diagram is a part of the UML for visualising important elements of a class and their relationship to each other. The AWG-Channel-Spacing tool basically consists of four classes:

- MainWindow
- Calculation
- Chart
- QCustomPlot

The class "MainWindow" is used to import the parameters mentioned in Section 3.4. Furthermore, functions such as saving and displaying the calculated parameters are implemented in this class. All calculations are carried out with the class "calculation". The QT signal and slot concept is used for communication between the classes. The signal "sendParameter()" from the class "MainWindow" sends the input parameters to the class "Calculation" and receives them with the slot "receiveParameter()". The calculation is started after receiving the parameters. The calculated parameters are sent back to the "MainWindow" with the signal "sendCalculatedParameter()". The received calculated parameters in the class "MainWindow" are displayed in the table, see Figure 3.2 "calculation of dxn". This algorithm is used for each of the three functions (table view, graphic view and save). For the graphical view, the calculated parameters are also emitted to the class "chart". The class "QCustomPlot" is responsible for the visualisation.

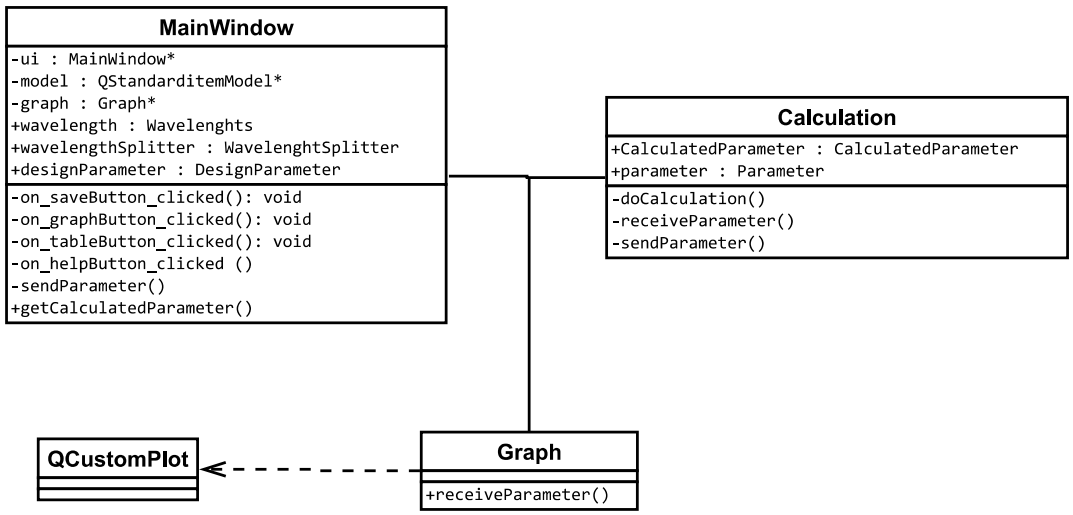

Figure 3.8: UML diagram.

4 Evaluation

In this section, the methods described in Section 2.1.1 – 2.1.3 and the correction of the methods in Section 2.2 are compared using a 20-channel 200-GHz AWG. The calculation and subsequent evaluation of this AWG is performed with Matlab [24].

The newly developed AWG-Channel-Spacing tool is tested with the same 20-channel 200-GHz AWG and with a 40-channel 100-GHz AWG to determine the correctness of the tool and verify that it provides the same results. In addition, the transmission parameters of the 20-channel 200-GHz AWG is compared before and after optimisation to determine whether the optimisation has an impact on the AWG performance.

4.1 Comparison of the Methods

Three different methods have been developed at the Vorarlberg University of Applied Sciences and their correction developed in this work to recalculate the dx-parameter to maintain a constant channel spacing in the frequency domain. For comparison, a 20-channel 200-GHz AWG is used. The same design parameters are used in all three methods and for correcting the methods. The results of the three methods according to the optimisation workflow presented in Section2 are shown in Figure 4.1. For calculation and graphical illustration Matlab is used. The result shows an almost constant channel spacing in the frequency domain for all three methods. This means that all the methods presented are suitable for optimisation and therefore the channel spacing corresponds to the ITU-Grid.

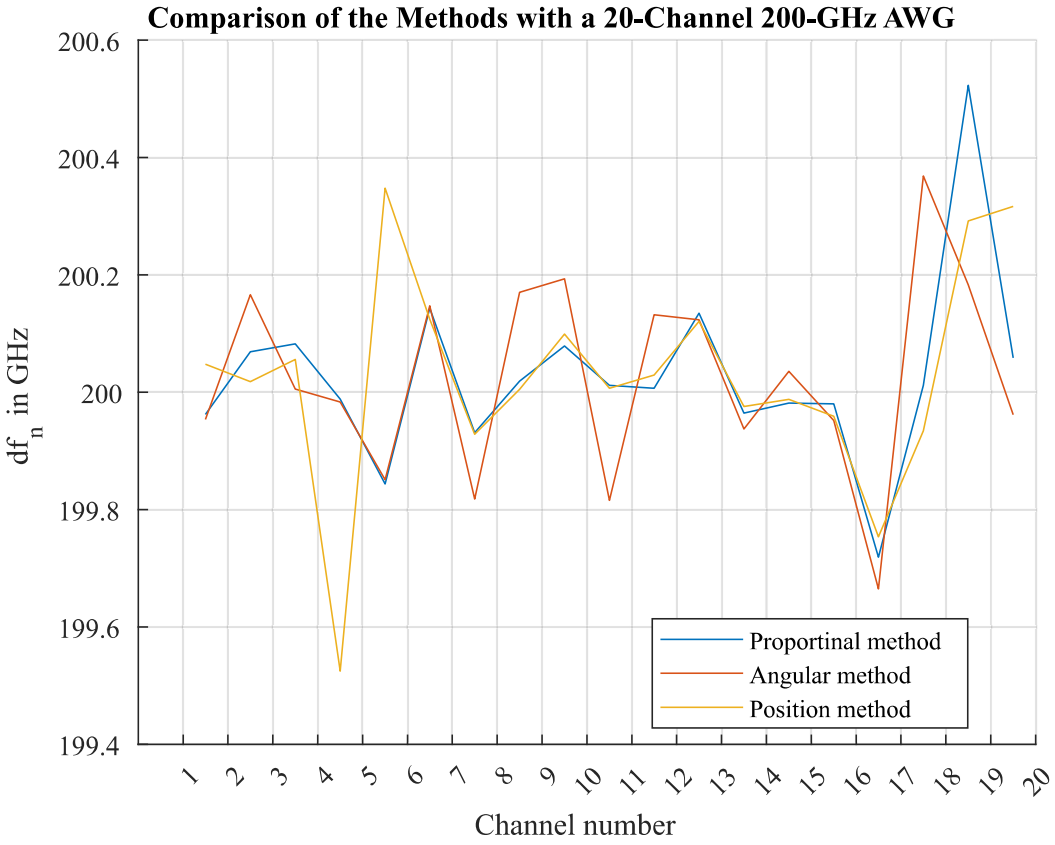

Figure 4.1: Comparison of the methods using a 20-channel 200-GHz AWG.

However, to demonstrate which is the most suitable choice, the average, the standard deviation, and the maximum deviation across all channels of the methods are calculated (see Table 4.1). The values of the maximum deviation consider the plus and minus 200 GHz direction. All values presented in the table are in GHz. The angular method provides on average the best approximation to 200 GHz and has the lowest maximum deviation across all channels. Consequently, it can be assumed that the angular method delivers the best results, although the difference to the other methods is minimal.

20-channel 200-GHz AWG	Average	Standard deviation	Max. deviation
Proportional method	200.0269	0.1549	0.5231
Angular method	200.0245	0.1699	0.3480
Position method	200.0278	0.1881	0.4752

Table 4.1: Comparison of the methods using a 20-channel 200-GHz AWG.

4.2 Verification of the AWG-Channel-Spacing Tool

The newly developed AWG-Channel-Spacing tool is verified with the same 20-channel 200-GHz AWG as in Section 4.1 to ensure that all functions of the tool operate correctly.

4.2.1 20-channel 200-GHz AWG

The calculation of the 20-channel 200-GHz AWG is performed using the proportional method. The result of the channel spacing in the wavelength domain ($d\lambda$) and in the frequency domain (df) is shown graphically in Figure 4.2. The graph is created using the AWG-Channel-Spacing tool. As provided by the ITU-Grid, the channel spacing in the frequency domain is almost constant, i.e. the trend is neither decreasing nor increasing. Additionally, the dx_n-values are calculated using Matlab to verify the correctness of the calculation. The dx_n-values calculated with Matlab and with the AWG-Channel-Spacing tool match each other.

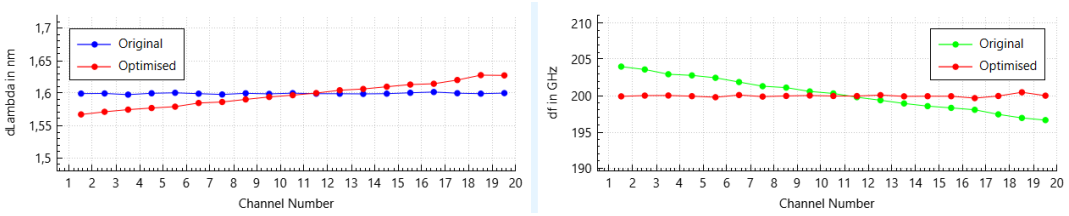

Figure 4.2: Original and optimised channel spacing of a 20-channel 200-GHz AWG.

4.3 Comparison of the Original to Optimised 20-channel 200-GHz AWG

To verify whether the transmission parameters changed before (original) and after the optimisation, the 20-channel 200-GHz AWG was evaluated. Table 4.2 shows the comparison of all transmission parameters described in Section 1.1.4.3. The original 20-channel 200-GHz AWG is simulated then technologically manufactured and measured. The optimised AWG is only simulated. The design can be found in Figure 5.1 in the appendix.

20-channel 200-GHz AWG	Original (Simulated)	Original (Measured)	Optimised (Simulated)
Peak insertion loss	-0.457 dB	-2.637 dB	-0.469 dB
Peak insertion loss uniformity	0.574 dB	0.608 dB	0.589 dB
Insertion loss	-1.814 dB	-3.172 dB	-1.834 dB
Insertion loss uniformity	0.610 dB	1.036 dB	0.638 dB
Adjacent channel crosstalk	41.418 dB	37.940 dB	37.333 dB
Non-adjacent channel crosstalk	52.729 dB	37.383 dB	53.703 dB
Background crosstalk	-60.584 dB	-60.462 dB	-59.371 dB

Table 4.2: Comparison of the original/optimised transmission parameters of a 20-channel 200-GHz AWG.

The insertion losses are slightly worse in the original (Measured), which can be attributed to the losses that occur when coupling from the fiber to the AWG. The peak insertion loss and the insertion loss uniformity are nearly the same in the comparison between the simulated original and optimised. There are small deviations in the crosstalk parameters, which is the result of the shift. In general, it can be determined that the shift of the parameter "separation of the output waveguides" has no significant influence on the performance of the AWG. All transmission parameters of the simulated and measured original 20-channel 200-GHz AWG and of the simulated optimised 20-channel 200-GHz AWG can be found in the appendix in Figure 5.2 - Figure 5.4.

5 Conclusion

The main goal of this master's thesis was the development of a software tool to calculate the channel spacing of an optical multiplexer/demultiplexer based on arrayed waveguide gratings in accordance to ITU-Grid standards. According to the ITU-Grid, the channel spacing should be constant in the frequency domain. This can be achieved by shifting the output waveguides (geometric parameter dx separation of the output waveguides), which leads to variable dx_n-values.

This work is divided into the following parts. An introduction to the theory of fibre optics and AWGs to understand the problem and a detailed description of the different parameters, which are used for the evaluation of an AWG. In addition, the specific development process of an AWG at the Vorarlberg University of Applied Sciences is demonstrated, which includes the simulation in Phasar tool and the evaluation with the AWG-Analyzer tool.

The concept for solving the problem was explained in section 2. The solution was achieved by shifting the position of the output waveguides. For the calculation of this shift, the proportional method, the angular method and the position method were used and were described in this section. In addition, the entire workflow of an AWG is shown and how this could be improved by using the AWG-Channel-Spacing tool.

The three methods and their optimisation were implemented in the AWG-Channel-Spacing tool which was developed in this thesis. This software tool and its functionality were described in Section 3. The software tool provides an easy user interface and the possibility to display the calculated parameters graphically and in a tabular format. This tool operates as an interface between the design process in Phasar tool and the evaluation process in the AWG-Analyzer tool and is able to import the data format from the AWG-Analyzer tool and return the data in a suitable data format for Phasar tool.

Beyond the given goals, two new and optimised calculation methods for the dx_n-values were introduced. These methods led to an almost constant result of the channel spacing in the frequency domain. Since both methods showed similar results, only one of them was implemented in the AWG-Channel-Spacing tool.

The evaluation of the methods of the AWG-Channel-Spacing tool and the comparison between original and optimised AWGs is discussed in Section 4. In comparison, the methods developed by the Vorarlberg University of Applied Science are relative similar regarding to channel spacing, whereby the angular method performs slightly better. The best results were achieved by the optimisation of the methods which was developed in this work. The AWG-Channel-Spacing tool was verified using a 20-channel 200-GHz AWG. The features such as saving the dx_n-values, the graphical representation and the tabular representation of the calculated parameters have been successfully implemented. As a result of this work, it has been shown that the optimisation of the channel spacing has almost no influence on the performance (transmission parameters) of the AWG.

Bibliography

[1] *Chapter 1, DWDM Overview*. [Online]. Available: https://docstore.mik.ua/univercd/cc/td/doc/product/ong/15400/r70docs/70epg/d7ovw.htm#wp1084162 (visited on 07/03/2022).

[2] G. Keiser, *Optical communications essentials* (McGraw-Hill networking professional). New York: McGraw-Hill, 2003, ISBN: 978-0-07-141204-9.

[3] B. P. S. Gaurav Kaushik Manish Sharma, "OPTICAL FIBER COMMUNICATION: (Advantages and Disadvantages)," ISSN: 2349-6002.

[4] A. D. F. Adnan Hussein Ali, "Design and Performance Analysis of the WDM Schemes for Radio over Fiber System With Different Fiber Propagation Losses," Feb. 2019. DOI: 10.3390/fib7030019.

[5] D. Seyringer and Society of Photo-optical Instrumentation Engineers, *Arrayed waveguide gratings*. 2016, ISBN: 978-1-5106-0359-2.

[6] N. Dr.Gaillan H.Abdullah Dr.Bushra.R.Mhdi, "Design Thin Film Narrow Band-pass Filters For Dense Wavelength Division Multiplexing," Jun. 2012, ISSN: 2252-8814.

[7] C. Massaroni, P. Saccomandi, and E. Schena, "Medical Smart Textiles Based on Fiber Optic Technology: An Overview," *Journal of Functional Biomaterials*, vol. 6, no. 2, pp. 204–221, Apr. 2015. DOI: 10.3390/jfb6020204.

[8] M. Dasan, F. Francis, K. T. Sarath, E. Dipin, and T. Srinivas, "Optically Multiplexed Systems: Wavelength Division Multiplexing," in *Multiplexing*, S. Mohammady, Ed., IntechOpen, Sep. 2019, ISBN: 978-1-78984-568-6. DOI: 10.5772/intechopen.88086.

[9] S. V. Kartalopoulos, *Introduction to DWDM technology: data in a rainbow*, eng. New York: IEEE Press, 2000, ISBN: 978-0-8194-3620-7.

[10] *FH Vorarlberg – University of Applied Sciences*. [Online]. Available: https://www.fhv.at/ (visited on 08/08/2022).

[11] *WDM Phasar Freeware*, en-US, Nov. 2013. [Online]. Available: https://optiwave.com/resources/academia/wdm-phasar-download/ (visited on 08/02/2022).

[12] D. Seyringer and P. Schmid, "A new software tool is developed to evaluate the measured/simulated transmission characteristics of optical multiplexers/demultiplexers," Marseille, France, Sep. 2011, p. 81671D. DOI: 10.1117/12.892462.

[13] Severin Keller, Dusko Vukovic, Stanislava Serecunova, Dana Seyringer, and Fiorention Valerio Conte, "AWG-Wuckler: A Novel Software Tool for Flexible Design of Arrayed Waveguide Gratings," Graz, Austria, 2022, pp. 1–6.

[14] P. Schmid, *Development of a software tool to evaluate simulated and measured transmission characteristics of optical multiplexers/demultiplexers based on arrayed waveguide gratings*, 2011.

[15] *G.694.2 : Spectral grids for WDM applications: CWDM wavelength grid.* [Online]. Available: https://www.itu.int/rec/T-REC-G.694.2/en (visited on 08/01/2022).

[16] *ITU Grid Specification (100GHz,50GHz at S,C,L Band) - Flipbook by ty40511 — FlipHTML5.* [Online]. Available: https://fliphtml5.com/atpiy/rzwt (visited on 08/01/2022).

[17] D. Seyringer and E. Hodzic, "Calculation of accurate channel spacing of an AWG optical demultiplexer applying proportional method," J.-M. Fédéli, Ed., Barcelona, Spain, Jun. 2015, 95200T. DOI: 10.1117/12.2178271.

[18] D. Seyringer, "Application of Angular Method to Correct Channel Spacing Between AWG Demultiplexed Channels," in *TechConnect Briefs 2016: Advanced Manufacturing*, Washington DC, May 2016, pp. 267–270.

[19] E. Hodzic, D. Seyringer, F. Uherek, J. Chovan, and A. Kuzma, "Calculation of accurate channel spacing of an arrayed waveguide grating optical multiplexer/demultiplexer applying position method," in *The Tenth International Conference on Advanced Semiconductor Devices and Microsystems*, Smolenice, Slovakia: IEEE, Oct. 2014, pp. 1–4, ISBN: 978-1-4799-5475-9.

[20] H.-Y. Kim, "Statistical notes for clinical researchers: Simple linear regression 2 – evaluation of regression line," *Restorative Dentistry & Endodontics*, vol. 43, no. 3, e34, 2018. DOI: 10.5395/rde.2018.43.e34.

[21] *Qt — Cross-platform software development for embedded & desktop*, en. [Online]. Available: https://www.qt.io (visited on 08/19/2022).

[22] J. Blanchette, M. Summerfield, and J. Blanchette, *C++ GUI Programmierung mit Qt 4: die offizielle Einführung* (Programmer's Choice), 2., aktualisierte Aufl. München: Addison Wesley, 2009, ISBN: 978-3-8273-2729-1.

[23] D. Molkentin, *Qt 4: Einführung in die Applikationsentwicklung* (Novice). München: Open Source Press, 2006, ISBN: 978-3-937514-12-3.

[24] *MATLAB - MathWorks - MATLAB & Simulink*. [Online]. Available: `https://de.mathworks.com/products/matlab.html` (visited on 07/04/2022).

Appendix

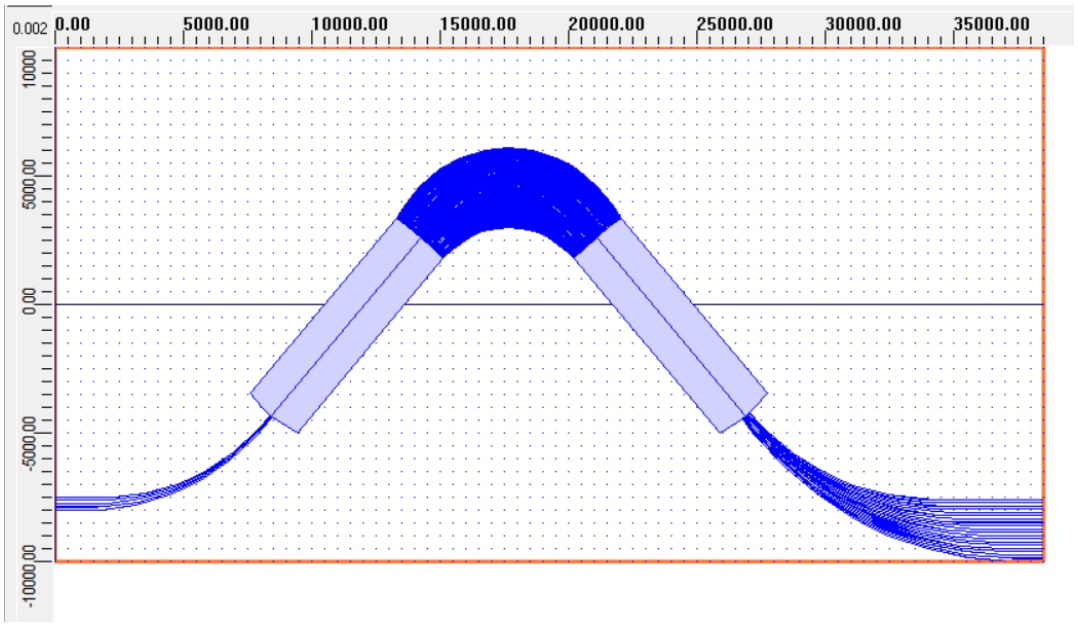

Figure 5.1: Designed 20-channel 200-GHz in Phasar tool.

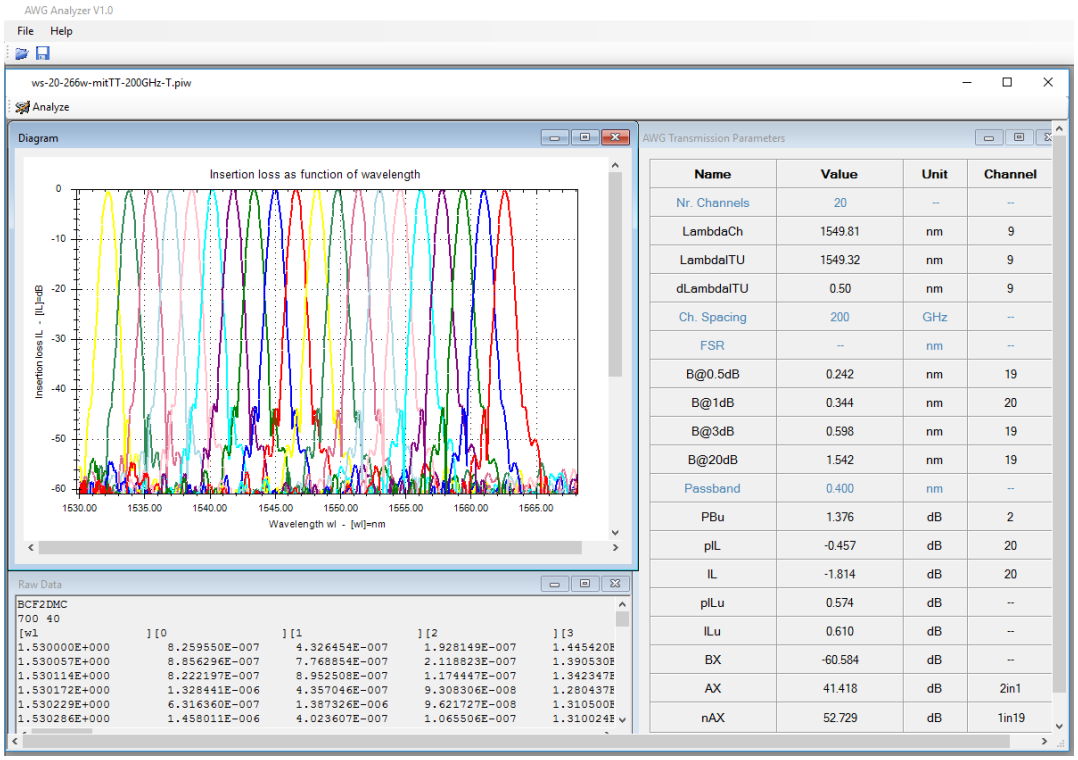

Name	Value	Unit	Channel
Nr. Channels	20	--	--
LambdaCh	1549.81	nm	9
LambdaITU	1549.32	nm	9
dLambdaITU	0.50	nm	9
Ch. Spacing	200	GHz	--
FSR	--	nm	--
B@0.5dB	0.242	nm	19
B@1dB	0.344	nm	20
B@3dB	0.598	nm	19
B@20dB	1.542	nm	19
Passband	0.400	nm	--
PBu	1.376	dB	2
pIL	-0.457	dB	20
IL	-1.814	dB	20
pILu	0.574	dB	--
ILu	0.610	dB	--
BX	-60.584	dB	--
AX	41.418	dB	2in1
nAX	52.729	dB	1in19

Figure 5.2: Transmission parameters of the simulated original 20-channel 200-GHz AWG.

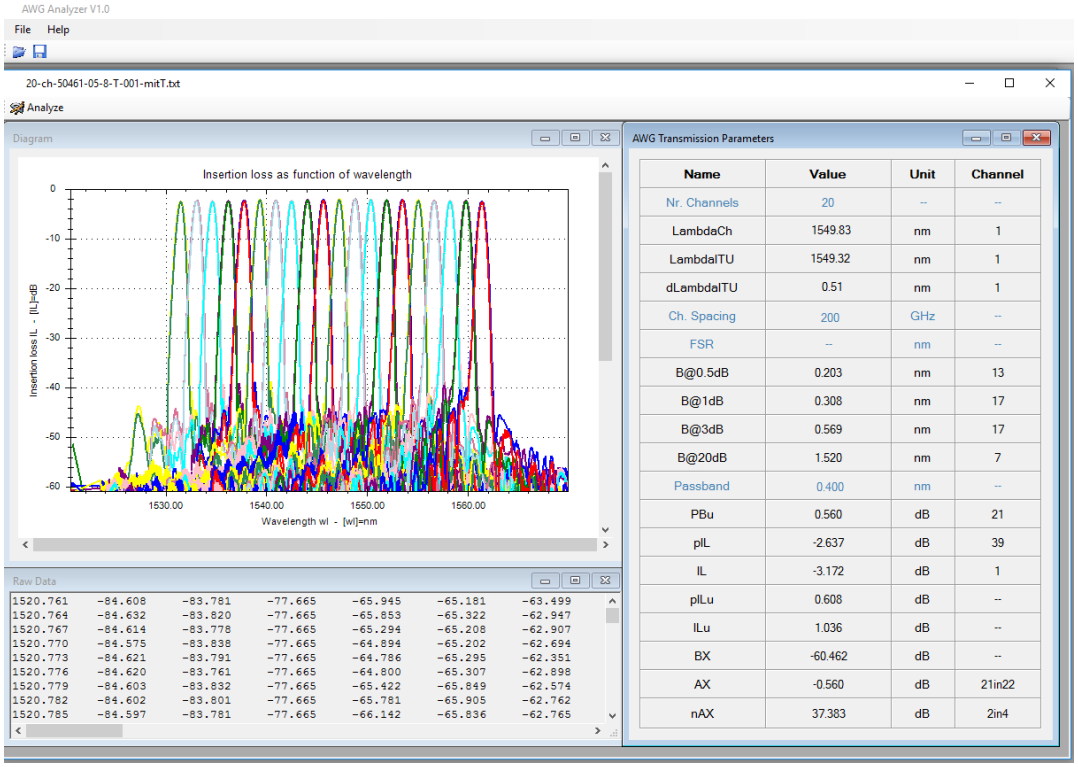

Name	Value	Unit	Channel
Nr. Channels	20	--	--
LambdaCh	1549.83	nm	1
LambdaITU	1549.32	nm	1
dLambdaITU	0.51	nm	1
Ch. Spacing	200	GHz	--
FSR	--	nm	--
B@0.5dB	0.203	nm	13
B@1dB	0.308	nm	17
B@3dB	0.569	nm	17
B@20dB	1.520	nm	7
Passband	0.400	nm	--
PBu	0.560	dB	21
pIL	-2.637	dB	39
IL	-3.172	dB	1
pILu	0.608	dB	--
ILu	1.036	dB	--
BX	-60.462	dB	--
AX	-0.560	dB	21in22
nAX	37.383	dB	2in4

Figure 5.3: Transmission parameters of the measured original 20-channel 200-GHz AWG.

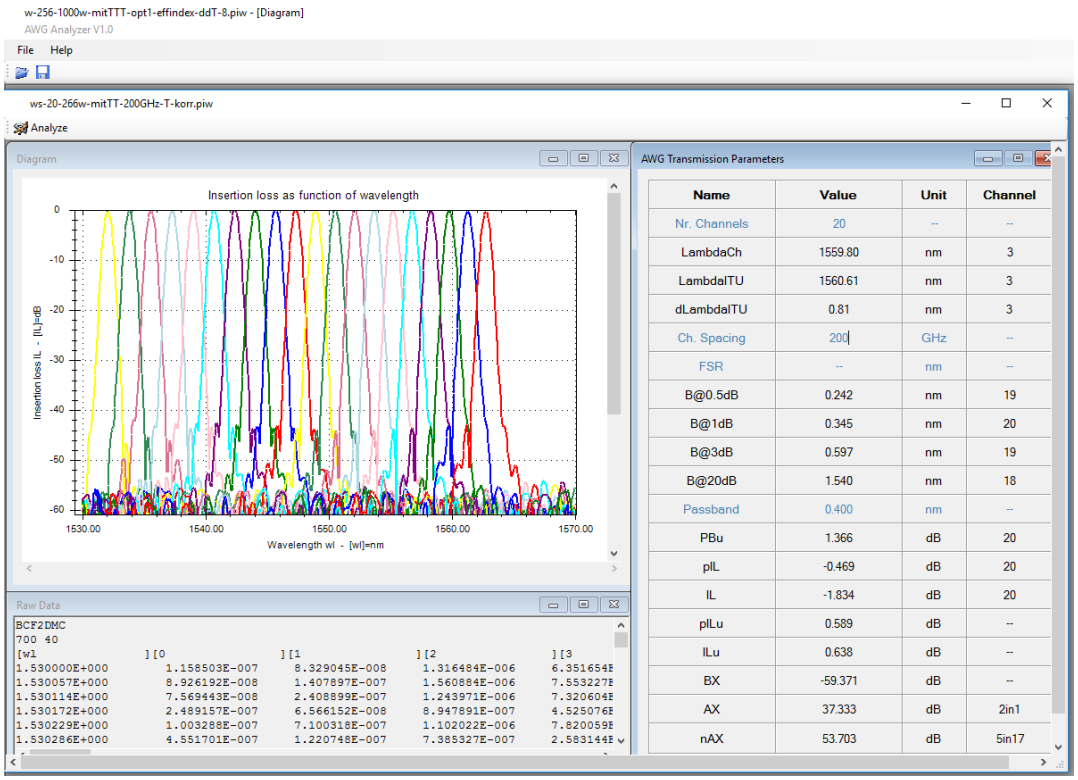

Name	Value	Unit	Channel
Nr. Channels	20	--	--
LambdaCh	1559.80	nm	3
LambdaITU	1560.61	nm	3
dLambdaITU	0.81	nm	3
Ch. Spacing	200	GHz	--
FSR	--	nm	--
B@0.5dB	0.242	nm	19
B@1dB	0.345	nm	20
B@3dB	0.597	nm	19
B@20dB	1.540	nm	18
Passband	0.400	nm	--
PBu	1.366	dB	20
pIL	-0.469	dB	20
IL	-1.834	dB	20
pILu	0.589	dB	--
ILu	0.638	dB	--
BX	-59.371	dB	--
AX	37.333	dB	2in1
nAX	53.703	dB	5in17

Figure 5.4: Transmission parameters of the simulated optimised 20-channel 200-GHz AWG.

Statement of Affirmation

I hereby declare that all parts of this thesis were exclusively prepared by me, without using resources other than those stated above. The thoughts taken directly or indirectly from external sources are appropriately annotated.

This thesis or parts of it were not previously submitted to any other academic institution and have not yet been published.

Dornbirn, 05. September 2022 Manuel Humpeler, BSc